Applied Numerical Mathematics 134 (2018) 81–104

Contents lists available at ScienceDirect

Applied Numerical Mathematics

www.elsevier.com/locate/apnum

Localized kernel-based approximation for pricing financial options under regime switching jump diffusion model

Reza Mollapourasl [a,b,*], Majid Haghi [a], Ruihua Liu [c]

[a] School of Mathematics, Shahid Rajaee Teacher Training University, Lavizan, Tehran 16788, Iran
[b] Department of Mathematics, Oregon State University, Corvallis, OR 97331, USA
[c] Department of Mathematics, The University of Dayton, 300 College Park, Dayton, OH 45469, USA

ARTICLE INFO

Article history:
Received 3 March 2018
Received in revised form 13 July 2018
Accepted 14 July 2018
Available online 18 July 2018

Keywords:
Radial basis functions
Finite difference
Option pricing
Regime-switching models
Jump diffusion
Operator splitting method
Convergence

ABSTRACT

In this paper, we consider European and American option pricing problems under regime switching jump diffusion models which are formulated as a system of partial integro-differential equations (PIDEs) with fixed and free boundaries. For free boundary problem arising in pricing American option, we use operator splitting method to deal with early exercise feature of American option. For developing a numerical technique we employ localized radial basis function generated finite difference (RBF-FD) approximation to overcome the ill-conditioning and high density issues of discretized matrices. The proposed method leads to linear systems with tridiagonal and diagonal dominant matrices. Also, in this paper the convergence and consistency of the proposed method are discussed. Numerical examples presented in the last section illustrate the robustness and practical performance of the proposed algorithm for pricing European and American options.

Published by Elsevier B.V. on behalf of IMACS.

1. Introduction

Unlike the standard Black–Scholes model [9] which assumes that the underlying assets follow a geometric Brownian motion with constant mean return and volatility, the rationale behind the regime switching framework is that the market may switch from time to time among different regimes. In short-term political or economic uncertainty, this property of regime switching model help us to account for certain periodic or cyclic patterns. In many practical researches such as [6] regime switching model has been used widely. Some of regime switching applications are in insurance [28], electricity markets [27,48], natural gas [13,1], valuation of stock loans [53], and interest rate dynamics [32].

Jumps are regularly observed in the discrete movement of stock price and these jumps can not be captured by the log normal distribution characteristic of the stock price in the Black Scholes model. Therefore an alternative model is necessary to overcome these issues. To resolve these issues several models have been proposed in the literature. Among these, the jump diffusion model introduced by Merton [39] and Kou [34] is one of the most used model. These models have finite jump activity, unlike the more general approach with possibly infinite jump activity proposed in [12]. The addition of jumps into the model generates heavy tails in returns for short time intervals, and allows large sudden changes in the underlying asset. This is also important from a risk management perspective, since the implication is that large losses are possible even in a short time interval.

In this study, we develop a numerical method to price European and American options under the regime switching jump diffusion model. The prices of European options under the regime switching jump diffusion model are derived by

* Corresponding author.
E-mail addresses: mollapour@srttu.edu (R. Mollapourasl), majidhaghi1363@gmail.com (M. Haghi), rliu01@udayton.edu (R. Liu).

https://doi.org/10.1016/j.apnum.2018.07.008
0168-9274/Published by Elsevier B.V. on behalf of IMACS.

solving a system of PIDEs, and the American options lead to solving a system of PIDEs with free boundaries. A variety of numerical methods are proposed to price an European or American option when the underlying asset follows a regime switching model. In [7] a global RBF collocation method for pricing the American options is presented. In [15] an explicit formula is derived as an expectation of Merton jump diffusion process, and a more general multinomial method is proposed for accommodate an arbitrary number of regimes and a generic jump size distribution, and is used for pricing American options. A modified trinomial tree model is considered in [52] for controlling the risk neutral probability measure in different regimes to ensure that the tree model can accommodate the data of all different regimes at the same time. In [33], a numerical scheme is developed via a combination of an implicit implementation of the θ-method and a penalty scheme for pricing American option under a regime switching model without jump diffusion.

Also, in [51] a second-order method based on exponential time differencing approach is obtained for solving American basket options under regime switching model. For dealing with free boundary problems, they use a penalty technique, and consistency and convergence of the proposed method are derived. An implicit method with three time levels is employed in [36] for solving the PIDE arisen for pricing options under regime switching model with jump diffusion process, and the operator splitting method is considered for evaluation American options and solving the equivalent linear complimentary problem. Optimal selling rules are considered in [18] for asset trading using a regime switching exponential Gaussian diffusion model. The derived optimization problem is solved by a combined method of boundary value problems and probabilistic analysis. Also, a method of upper and lower solutions for a regime switching model is obtained in [17], then by using this method authors prove the existence of a unique C^2 solution of the associated system of ordinary differential equations with two-point boundary conditions.

The regime switching recombining tree method for pricing options on a single asset is proposed in [37], and then generalized to options with two correlated underlying assets whose prices are governed by the regime switching geometric Brownian motion models in [38]. Then the weak convergence of the discrete lattice approximations to the continuous-time regime switching diffusion processes is discussed. In [19] authors provide an explicit finite difference scheme for the differential operator and four-points open type formula for integral operator to price European options under Bates model. Two algorithms for pricing of European options in a regime switching jump diffusion model are developed in [22] based on theoretical analysis for convergence of the algorithms which is carried out in [21]. Also, in [43] the authors consider a numerical algorithm based on finite element method to approximate the spatial terms of the option pricing equations using linear and quadratic basis polynomial approximations and for time discretization, they use exponential time integration technique. A finite element method and Chebyshev pseudospectral approximation are employed for pricing American options on an underlying described by the Bates model in [5,3] and they used a Richardson extrapolation technique to reduce the problem with fixed boundary. Also, method of lines algorithm is used in [14] for numerical evaluation of American call options under stochastic volatility and jump-diffusion.

Kernel based meshfree methods are of efficient tools for solving PDEs and integral equations, and especially in [4,20], meshfree methods based on RBF approximation have been shown to perform better than finite difference methods for option pricing problems in one and two spatial dimensions. However, all of these papers employ global RBF collocation methods which lead to the dense linear systems, and computational costs that become prohibitive as the number of dimensions increase. Localized RBF approximations such as the RBF partition of unity collocation method (RBF-PUM) and RBF-FD give an answer to deal with these issues. In [41,40], the authors price American and European options under Heston's stochastic volatility and jump diffusion models using RBF-PUM applied to a linear complementary formulation of the free boundary partial differential equation problem.

RBF-FD method has been implemented in various favors and contexts in the last ten years, the first survey articles on RBF-FD are just emerging in [23,24]. The matrices formed during the localized RBF-FD method will be sparse and, hence, will not suffer from ill-conditioning and high computational costs. In the present paper, we use RBF-FD method for differential operator approximation of the system of partial integro-differential equations arisen in European and American option pricing problems under the regime switching model. In addition, for American option we apply operator splitting method which has been used in [29] for solving the free boundary problem.

In the next section, we introduce the regime switching model with jump diffusion and a system of partial integro-differential equations for pricing European option, then we formulate the American option pricing problem as a free boundary value problem. Then operator splitting method is used to convert the free boundary value problem to a problem with fixed boundaries. For time discretization, we use a three-level implicit-explicit time discretization that treats the non-local integral term explicitly in section 3, and then RBF-FD approximation is introduced and applied for derivative approximation, and also discretization of integral term is prepared for full discretization in section 4. Convergence and consistency analysis of proposed method are proved in section 5 to grantee the applicability of the algorithm. Finally, in the last section, the accuracy and efficiency of the proposed method is numerically investigated for European and American options, and compared with existing methods in the literature.

2. Regime-switching jump diffusion model

Consider a complete filtered probability space $(\Omega, \mathcal{F}, (\mathcal{F})_{t\in[0,T]}, \mathbb{P})$ and $T > 0$ is a fixed finite time horizon. We suppose that the underlying asset switches among a finite number of states $\mathcal{M} := \{1, 2, 3, ..., m\}$, which is modeled by a continuous-

time Markov chain process $\{\alpha_t\}_{t\in[0,T]}$. Then we have the regime generator of the Markov chain $\{\alpha_t\}_{t\in[0,T]}$ by an $m\times m$ matrix

$$\mathbf{Q}=\begin{pmatrix} q_{11} & \dots & q_{1m} \\ \dots & \dots & \dots \\ q_{m1} & \dots & q_{mm} \end{pmatrix}. \tag{1}$$

From Markov chain theory [50], the entries of generator matrix satisfy

- $q_{ij}\geq 0$ if $i\neq j$.
- $\sum_{j=1}^{m} q_{ij}=0$ for each $i\in\mathcal{M}$.

Assume that there exists an equivalent martingale measure $\mathbb{Q}$ under which the dynamics of the asset price are given by the following stochastic differential equation (SDE) as in [11,16]

$$\frac{\mathrm{d}S_t}{S_{t-}}=(r_{\alpha_t}-q_{\alpha_t}-\lambda_{\alpha_t}\kappa_{\alpha_t})\mathrm{d}t+\sigma_{\alpha_t}\mathrm{d}W(t)+(y_{\alpha_t}-1)\mathrm{d}N_t, \tag{2}$$

where W is a standard $\mathbb{Q}$-Brownian motion, N is an independent Poisson process with intensity rate $\lambda_{\alpha_t}=\lambda_i>0$ for each economic regime i of α_t, $\kappa_{\alpha_t}=\kappa_i$ is the expected value of the random value $y_{\alpha_t}-1=(y_i-1)$ of the jump size distribution producing a jump from S_{t-} to y_iS_{t-}. The parameters $r_{\alpha_t}=r_i$, $q_{\alpha_t}=q_i$ and $\sigma_{\alpha_t}=\sigma_i(>0)$, stand for the risk free interest rate, the continuous dividend yield and the volatility, respectively. In this paper we focus on two popular jump-diffusion models with finite activity, Merton's [39] and Kou's [34] model. Hence, the density function and corresponding expectation of the impulse function for Merton's model with mean μ_i^J and standard deviation σ_i^J are given by

$$f(y,i)=\frac{1}{\sigma_i^J\sqrt{2\pi}}\exp\left[-\left(\frac{y-\mu_i^J}{\sqrt{2}\sigma_i^J}\right)^2\right],\qquad \kappa_i=\exp(\mu_i^J+\frac{(\sigma_i^J)^2}{2})-1, \tag{3}$$

with $\sigma_i^J>0$, $\mu_i^J\in\mathbb{R}$, and for Kou's model are defined by

$$f(y,i)=p\eta_1e^{-\eta_1 y}\mathcal{H}(y)+(1-p)\eta_2e^{\eta_2 y}\mathcal{H}(-y),\qquad \kappa_i=p\frac{\eta_1}{\eta_1-1}+(1-p)\frac{\eta_2}{\eta_2+1}-1, \tag{4}$$

with $\eta_1>1$, $\eta_2>0$, $0<p<1$ and $\mathcal{H}(\cdot)$ is the Heaviside function.

Let $V(t,S,i)$ denote the price of an European option when the underlying asset S_t follows the regime switching jump diffusion model with the no arbitrage condition in (2), so the price of a European option $V(t,S,i)$ satisfies the system of partial integro-differential equations (PIDEs)

$$\begin{aligned}\frac{\partial V(t,S,i)}{\partial t}+\frac{\sigma_i^2S^2}{2}\frac{\partial^2V(t,S,i)}{\partial S^2}+(r_i-q_i-\lambda_i\kappa_i)S\frac{\partial V(t,S,i)}{\partial S}-(r_i+\lambda_i)V(t,S,i)\\ +\lambda_i\int_0^\infty V(t,Sy,i)\psi(y,i)dy+\sum_{j=1}^{m}q_{ij}V(t,S,j)=0,\end{aligned} \tag{5}$$

for all $(t,S,i)\in[0,T)\times[0,\infty)\times\mathcal{M}$ with the terminal condition

$$V(T,S,i)=g(S) \tag{6}$$

where T is the time to maturity, and $g(S)$ is known as payoff function and defined by $\max(K-S,0)$ for put options and $\max(S-K,0)$ for call options, and K is the exercise price. Also, ψ is a density function for jump size.

Now, we consider the transformations $x=\log(\frac{S}{K})$ and $\tau=T-t$, and let $u(\tau,x,i)=V(T-\tau,Ke^x,i)$, denoted as the value of an option on the transformed space x for the ith regime, so $u(\tau,x,i)$ satisfies the system of PIDEs

$$\frac{\partial u(\tau,x,i)}{\partial\tau}-\mathcal{D}_iu(\tau,x,i)-\lambda_i\mathcal{J}_iu(\tau,x,i)-\sum_{j=1}^{m}q_{ij}u(\tau,x,j)=0,\quad i\in\mathcal{M} \tag{7}$$

with initial condition

$$u(0,x,i)=g(Ke^x), \tag{8}$$

for all $(\tau,x,i)\in(0,T]\times\mathbb{R}\times\mathcal{M}$ where

$$\mathcal{D}_i u(\tau,x,i) := \frac{\sigma_i^2}{2}\frac{\partial^2 u(\tau,x,i)}{\partial x^2} + (r_i - q_i - \frac{\sigma_i^2}{2} - \lambda_i\kappa_i)\frac{\partial u(\tau,x,i)}{\partial x} - (r_i+\lambda_i)u(\tau,x,i), \tag{9}$$

$$\mathcal{J}_i u(\tau,x,i) := \int_{-\infty}^{\infty} u(\tau,y,i) f(y-x,i)dy. \tag{10}$$

In order to develop a numerical scheme for PIDEs (7), we need to impose some boundary conditions, so let the asymptotic behavior of the European call option as

$$\lim_{x\to-\infty} u(\tau,x,i) = 0, \quad \lim_{x\to\infty}[u(\tau,x,i) - K(e^{x-q_i\tau} - e^{-r_i\tau})] = 0, \tag{11}$$

and the asymptotic behavior of the European put option is defined by

$$\lim_{x\to-\infty}[u(\tau,x,i) - K(e^{-r_i\tau} - e^{x-q_i\tau})] = 0, \quad \lim_{x\to\infty} u(\tau,x,i) = 0. \tag{12}$$

For the numerical purposes, first we localize the unbounded domain in $x\in(-\infty,\infty)$ direction with a bounded domain $[x_{\min}, x_{\max}]$, so for boundary conditions of European call option we have

$$u(\tau,x_{\min},i) = 0, \quad u(\tau,x_{\max},i) = K(e^{x_{\max}-q_i\tau} - e^{-r_i\tau}), \tag{13}$$

and for European put option, boundary conditions are defined by

$$u(\tau,x_{\min},i) = K(e^{-r_i\tau} - e^{x_{\min}-q_i\tau}), \quad u(\tau,x_{\max},i) = 0. \tag{14}$$

In the following, we will give the system of PIDEs formulation to price an American option under regime switching jump diffusion model. An American option has the early exercise feature, so the optimal exercise boundary is a free boundary and separates the stopping and continuation region. Let $V(t,S,i)$ denote the fair value of an American put option at time t if the asset price at that time is $S_t = S$, so $V(t,S,i)$ satisfy the following free boundary value problem

$$\begin{cases} \frac{\partial V(t,S,i)}{\partial t} + \frac{\sigma_i^2 S^2}{2}\frac{\partial^2 V(t,S,i)}{\partial S^2} + (r_i - q_i - \lambda_i\kappa_i)S\frac{\partial V(t,S,i)}{\partial S} - (r_i+\lambda_i)V(t,S,i) & \\ \quad +\lambda_i\int_0^\infty V(t,Sy,i)\psi(y,i)dy + \sum_{j=1}^m q_{ij}V(t,S,j) = 0 & S > S_i^F(t) \\ V(t,S,i) = K - S, & 0 \le S \le S_i^F(t), \\ V(T,S,i) = g(S), & \\ \lim_{S\to\infty} V(t,S,i) = 0, & \\ \lim_{S\to S_i^F(t)} V(t,S,i) = K - S_i^F(t), & \\ \lim_{S\to S_i^F(t)} \frac{\partial V(t,S,i)}{\partial S} = -1, & \\ S_i^F(T) = K, & \end{cases} \tag{15}$$

where $g(S)$ is the payoff function, and $S_i^F(t)$ for $i\in\mathcal{M}$ denote the unknown free moving exercise boundaries of the option. For solving the free boundary problem (15), there are some techniques such as linear programming [10], operator splitting method [29] penalty method which has been presented in [54,44,47].

In this work, we employ operator splitting method which has an advantage that the free boundary $S_i^F(t)$ does not explicitly appear in the problem formulation which later enables numerical discretization. Now, first we use the transformations $x = \log(\frac{S}{K})$ and $\tau = T - t$ similar to the European option, and let $u(\tau,x,i) = V(T-\tau, Ke^x, i)$, denoted as the value of an American option on the transformed space x for the ith regime, then $u(\tau,x,i)$ satisfies the following linear complementary problem (LCP) [46]

$$\begin{cases} \frac{\partial u(\tau,x,i)}{\partial\tau} - \mathcal{D}_i u(\tau,x,i) - \lambda_i\mathcal{J}_i u(\tau,x,i) - \sum_{j=1}^m q_{ij}u(\tau,x,j) \ge 0, \\ u(\tau,x,i) \ge g(Ke^x), \\ \left(\frac{\partial u(\tau,x,i)}{\partial\tau} - \mathcal{D}_i u(\tau,x,i) - \mathcal{J}_i u(\tau,x,i) - \sum_{j=1}^m q_{ij}u(\tau,x,j)\right)(u(\tau,x,i) - g(Ke^x)) = 0, \end{cases} \tag{16}$$

for all $(\tau,x,i)\in(0,T]\times(-\infty,\infty)\times\mathcal{M}$.

3. Time discretization

Let $\triangle\tau = \frac{T}{M}$ with integer $M \geq 1$ be a given time step and let the corresponding temporal grid points be given by $\tau_k = k\triangle\tau$ for $0 \leq k \leq M$. We apply an implicit-explicit (IMEX) time semi-discretization with three time levels to the PIDE (7). In particular, we consider the Crank–Nicolson–Leap–Frog (CNLF) scheme as in [2] and [31]. In [45] this type of scheme is called the IMEX-midpoint scheme. The differential part is treated implicitly, while the integral part is treated explicitly. In order to start the algorithm we will need initial data for $k = 0$ and the value for $k = 1$ is obtained by an implicit-explicit backward difference method of order one (IMEX-BDF1). Thus, let $U_i^k := u(\tau_k, x, i)$, the PIDE (7) for the price of an European option is approximated by following time semi-discrete scheme

$$\frac{U_i^1 - U_i^0}{\triangle\tau} = \mathcal{D}_i U_i^1 + \lambda_i \mathcal{J}_i U_i^0 + \sum_{j=1}^{m} q_{ij} U_j^1, \tag{17}$$

$$\frac{U_i^{k+1} - U_i^{k-1}}{2\triangle\tau} = \mathcal{D}_i\left(\frac{U_i^{k+1} + U_i^{k-1}}{2}\right) + \lambda_i \mathcal{J}_i U_i^k + \sum_{j=1}^{m} q_{ij}\left(\frac{U_j^{k+1} + U_j^{k-1}}{2}\right), \quad i \in \mathcal{M},\ 1 \leq k \leq M-1 \tag{18}$$

with initial condition

$$U_i^0(x) = g(Ke^x), \ \text{ for } x \in [x_{\min}, x_{\max}],$$

and boundary conditions for European call and put options are (13) and (14), respectively.

For American options, we employ and generalize operator splitting method which was introduced and applied for Black–Scholes model in [29] for solving LCP (16). By using an auxiliary function $\Upsilon(\tau, x, i)$, we can reformulate LCP (16) as

$$\begin{cases} \frac{\partial u(\tau,x,i)}{\partial \tau} - \mathcal{D}_i u(\tau,x,i) - \lambda_i \mathcal{J}_i u(\tau,x,i) - \sum_{j=1}^{m} q_{ij} u(\tau,x,j) = \Upsilon(\tau,x,i), \quad \Upsilon(\tau,x,i) \geq 0 \\ u(\tau,x,i) \geq g(Ke^x), \\ \Upsilon(\tau,x,i)(u(\tau,x,i) - g(Ke^x)) = 0, \end{cases} \tag{19}$$

for all $(\tau, x, i) \in (0, T] \times (-\infty, \infty) \times \mathcal{M}$. Each time step is split into two parts. Let $\Upsilon_i^k := \Upsilon(\tau_k, x, i)$ and start from the initial value U_i^0 and $\Upsilon_i^0 := 0$. First, the intermediate solution $\widetilde{U}_i^{k+1}$ is solved from the modified semi-discrete system of equations

$$\begin{cases} \frac{\widetilde{U}_i^1 - U_i^0}{\triangle\tau} - \mathcal{D}_i \widetilde{U}_i^1 - \lambda_i \mathcal{J}_i U_i^0 - \sum_{j=1}^{m} q_{ij} \widetilde{U}_j^1 = \Upsilon_i^0, \\ \Upsilon_i^1 = \Upsilon_i^0 + \frac{U_i^1 - \widetilde{U}_i^1}{\triangle\tau}, \\ \Upsilon_i^1 \geq 0,\ U_i^1 \geq g(Ke^x),\ \Upsilon_i^1(U_i^1 - g(Ke^x)) = 0, \end{cases} \tag{20}$$

and

$$\begin{cases} \frac{\widetilde{U}_i^{k+1} - U_i^{k-1}}{2\triangle\tau} - \mathcal{D}_i\left(\frac{\widetilde{U}_i^{k+1} + U_i^{k-1}}{2}\right) - \lambda_i \mathcal{J}_i U_i^k - \sum_{j=1}^{m} q_{ij}\left(\frac{\widetilde{U}_j^{k+1} + U_j^{k-1}}{2}\right) = \Upsilon_i^k, \\ \Upsilon_i^{k+1} = \Upsilon_i^k + \frac{U_i^{k+1} - \widetilde{U}_i^{k+1}}{2\triangle\tau}, \\ \Upsilon_i^{k+1} \geq 0,\ U_i^{k+1} \geq g(Ke^x),\ \Upsilon_i^{k+1}(U_i^{k+1} - g(Ke^x)) = 0, \end{cases} \tag{21}$$

with initial condition

$$U_i^0(x) = g(Ke^x), \ \text{ for } x \in [x_{\min}, x_{\max}],$$

for American put option boundary conditions are

$$U_i^k(x_{\min}) = K, \quad U_i^k(x_{\max}) = 0, \ \text{ for } 1 \leq k \leq M,$$

and for American call option boundary conditions will be

$$U_i^k(x_{\min}) = 0, \quad U_i^k(x_{\max}) = K, \ \text{ for } 1 \leq k \leq M.$$

4. RBF-FD approximation

Consider a spatial domain $\Omega \subset \mathbb{R}^d$ and a set of distinct points $\mathbf{X} = \{\mathbf{x}_1, \mathbf{x}_2, ..., \mathbf{x}_N\}$ in Ω. Also, let $\phi : \Omega \times \Omega \to \mathbb{R}$ be a kernel with the property $\phi(\mathbf{x}, \mathbf{y}) := \phi(||\mathbf{x} - \mathbf{y}||)$ for $\mathbf{x}, \mathbf{y} \in \Omega$, and $||\cdot||$ is the Euclidean norm. Kernels with this property known as radial functions. The RBF interpolant for a continuous target function $u : \Omega \to \mathbb{R}$ known at the nodes in $\mathbf{X}$ takes the form

$$\mathcal{I}_u(\mathbf{x}) = \sum_{j=1}^{N} \gamma_j \phi(||\mathbf{x} - \mathbf{x}_j||). \tag{22}$$

The interpolation coefficients $\{\gamma_j\}_{j=1}^N$ are determined by collocating the interpolant $\mathcal{I}_u(\mathbf{x})$ to satisfy the interpolation condition $\mathcal{I}_u(\mathbf{x}_i) = u(\mathbf{x}_i)$ for $i = 1, 2, ..., N$. This results in a symmetric system of linear equations

$$\underbrace{\begin{pmatrix} \phi(||\mathbf{x}_1 - \mathbf{x}_1||) & \phi(||\mathbf{x}_1 - \mathbf{x}_2||) & \cdots & \phi(||\mathbf{x}_1 - \mathbf{x}_N||) \\ \phi(||\mathbf{x}_2 - \mathbf{x}_1||) & \phi(||\mathbf{x}_2 - \mathbf{x}_2||) & \cdots & \phi(||\mathbf{x}_2 - \mathbf{x}_N||) \\ \vdots & \vdots & \ddots & \vdots \\ \phi(||\mathbf{x}_N - \mathbf{x}_1||) & \phi(||\mathbf{x}_N - \mathbf{x}_2||) & \cdots & \phi(||\mathbf{x}_N - \mathbf{x}_N||) \end{pmatrix}}_{\mathbf{A}} \underbrace{\begin{pmatrix} \gamma_1 \\ \gamma_2 \\ \vdots \\ \gamma_N \end{pmatrix}}_{\boldsymbol{\gamma}} = \underbrace{\begin{pmatrix} u_1 \\ u_2 \\ \vdots \\ u_N \end{pmatrix}}_{\mathbf{u}}. \tag{23}$$

When the points in $\mathbf{X}$ are chosen to be distinct and ϕ is a positive-definite radial kernel or an order one conditionally positive-definite kernel on $\mathbb{R}^d$, the coefficient matrix $\mathbf{A}$ is guaranteed to be non-singular, see [49]. Now, assume that $u : \Omega \to \mathbb{R}$ is a differentiable function. Also, let $\mathcal{D}$ as a linear differential operator. We want to approximate $\mathcal{D}u$ at scattered grids $\mathbf{X}$ with finite-difference-style local approximations. Consider any subset of $\mathbf{X}$ denoted by $\Omega_i = \{\mathbf{x}_1, ..., \mathbf{x}_n\}$ containing $n \ll N$ nodes which are nearest neighbors to $\mathbf{x}_i$ measured by Euclidean distance in $\mathbb{R}^d$. We refer to Ω_i as the stencil corresponding to $\mathbf{x}_i$. Approximation to $\mathcal{D}u$ at $\mathbf{x}_i$ involves a linear combination of the values of u over the stencil Ω_i of the form

$$\mathcal{D}(u(\mathbf{x}_i)) \approx \sum_{j=1}^{n} w_j u(\mathbf{x}_j), \tag{24}$$

where weights $\{w_j\}_{j=1}^n$ can be computed by RBFs, so this technique known as RBF-FD. We can rewrite (24) as $\mathcal{D}(u(\mathbf{x}_i)) \approx \mathbf{w}_i \mathbf{u}_i$, where $\mathbf{w}_i = [w_1, w_2, \ldots, w_n]^\top$ and $\mathbf{u}_i = [u_1, u_2, \ldots, u_n]^\top$, so for computing RBF-FD weights, first of all, we prepare a local interpolant

$$\mathcal{I}_u(\mathbf{x}) = \sum_{j=1}^{n} \gamma_j \phi(||\mathbf{x} - \mathbf{x}_j||), \tag{25}$$

and matrix-vector form of this relation is $\mathbf{A}_i \boldsymbol{\gamma}_i = \mathbf{u}_i$, where $\mathbf{A}_i$ is the local distance matrix and $\boldsymbol{\gamma}_i = [\gamma_1, \gamma_2, \ldots, \gamma_n]^\top$ and $\mathbf{u}_i$ is the known data corresponding to stencil of $\mathbf{x}_i$, respectively. Unknown coefficients $\boldsymbol{\gamma}_i$ are determined by $\boldsymbol{\gamma}_i = \mathbf{A}_i^{-1} \mathbf{u}_i$. Now, we apply the differentiation operator $\mathcal{D}$ to the both side of (25), then we have

$$\mathcal{D}(\mathcal{I}_u(\mathbf{x})) = \sum_{j=1}^{n} \gamma_j \mathcal{D}(\phi(||\mathbf{x} - \mathbf{x}_j||)). \tag{26}$$

Now, by collocating (26) at $\mathbf{x}_i$ and writing matrix-vector form, we derive

$$\mathcal{D}(u(\mathbf{x}_i)) = \mathcal{D}\Phi(\mathbf{x}_i)\boldsymbol{\gamma}_i = \mathcal{D}\Phi(\mathbf{x}_i)\mathbf{A}_i^{-1}\mathbf{u}_i, \tag{27}$$

where $\mathcal{D}\Phi(\mathbf{x}_i) = [\mathcal{D}\phi(||\mathbf{x}_i - \mathbf{x}_1||), \mathcal{D}\phi(||\mathbf{x}_i - \mathbf{x}_2||), ..., \mathcal{D}\phi(||\mathbf{x}_i - \mathbf{x}_n||)]$. By comparing (24) with (27), we conclude $\mathbf{w}_i = \mathcal{D}\Phi(\mathbf{x}_i)\mathbf{A}_i^{-1}$.

Global RBF method for deriving differentiation matrix needs $O(N^3)$ operations, and leads to a dense matrix, but in RBF-FD method for each stencil, we need $O(n^3)$ operations and there are N such stencils, so that the total cost of computing is $O(n^3 N)$, although we do not take into account the cost of determining the stencil grids. Since $n \ll N$ and n is fixed as N increases, so that the total cost will be $O(N)$. For computing weights, we need to compute the inverse of local distance matrix of order $n \times n$ for each stencil, and since distance matrix depends only on distance of grid points, in uniform grids which we use in this study, we only need to compute the inverse of local distance matrix once. Also, since computing differentiation matrix for each stencil is independent to other stencils, so parallel algorithms can be employed to increase the efficiency of RBF-FD method in high dimensional problems and adaptive algorithms.

4.1. Spatial discretization

For spatial discretization, we replace the unbounded domain $\{(\tau, x) \mid \tau \in (0, T], x \in \mathbb{R}\}$ with a bounded one $(0, T] \times [x_{\min}, x_{\max}]$ where the values $x_{\min}$ and $x_{\max}$, will be chosen based on standard financial arguments, such that the error caused by truncating the solution domain is negligible. Let $X = \{x_0, x_1, ..., x_{N_x}\} \subset [x_{\min}, x_{\max}]$ such that $x_{\min} = x_0 < x_1 < \ldots < x_{N_x} = x_{max}$, and $h = x_{j+1} - x_j$ for $j = 0, \ldots, N_x - 1$. For each point x_j, we choose an influence domain $X_j = \{x_1, x_2, ..., x_n\} \subset X$ which contains a local region formed by the n closest neighboring interpolation points to x_j. Local RBF interpolant for each regime is defined by

$$u(\tau_k, x, i) \approx \sum_{l=1}^{n} \gamma_l \phi(\|x - x_l\|) \tag{28}$$

where unknown $\{\gamma_l\}_{l=1}^{n}$ are determined by imposing the interpolation conditions and solving linear system of equations $\mathbf{\Phi}^j \boldsymbol{\gamma}^j = \mathbf{u}_i^j$, where $\mathbf{\Phi}^j = [\phi(\|x_i - x_k\|)]_{1 \le i,k \le n}$, $\boldsymbol{\gamma}^j = [\gamma_1, \gamma_2, ..., \gamma_n]^T$ and $\mathbf{u}_i^j = [u(\tau_k, x_1, i), u(\tau_k, x_2, i), ..., u(\tau_k, x_n, i)]^T$, regarding to this fact that $\mathbf{\Phi}^j$ is invertible, so we have $\boldsymbol{\gamma}^j = (\mathbf{\Phi}^j)^{-1} \mathbf{u}_i^j$.

For each interior point $x_j \in X$ we apply differential operator (9) to the local interpolant (28), so we have

$$\mathcal{D}_i u(\tau_k, x_j, i) = \sum_{l=1}^{n} \gamma_l \mathcal{D}_i \phi(\|x_j - x_l\|) =: \mathbf{D}_i^j \mathbf{u}_i^j \tag{29}$$

where

$$\mathbf{D}_i^j = [\mathcal{D}_i \phi(\|x_j - x_1\|), \mathcal{D}_i \phi(\|x_j - x_2\|), ..., \mathcal{D}_i \phi(\|x_j - x_n\|)](\mathbf{\Phi}^j)^{-1}. \tag{30}$$

Note that the influence domain for all the interior points is the same. Hence, $\mathbf{\Phi}^j$ is the same for all interior points and thus needs to be computed only once, and the computational efficiency can be improved. $\mathbf{D}_i^j$ is the local differentiation matrix, by inserting zeros in the proper locations, global differentiation matrix $\mathbf{D}_i$ is derived.

4.2. Discretization of the integral operator

To approximate the integral operator $\mathcal{J}_i$ numerically, let $\Omega = [x_{\min}, x_{\max}]$. So, we divide the integral into two parts on Ω and $\mathbb{R} \backslash \Omega$, so we have

$$\mathcal{J}_i u(\tau, x, i) = \int_{\Omega} u(\tau, y, i) f(y - x, i) dy + \int_{\mathbb{R} \backslash \Omega} u(\tau, y, i) f(y - x, i) dy \tag{31}$$

Let $R(\tau, x, i) = \int_{\mathbb{R} \backslash \Omega} u(\tau, y, i) f(y - x, i) dy$ and by using the boundary conditions for European put option we can calculate $R(\tau, x, i)$ by

$$R(\tau, x, i) = \int_{-\infty}^{x_{\min}} (K e^{-r_i \tau} - K e^{y - q_i \tau}) f(y - x, i) dy,$$

where for Merton model we have

$$R(\tau, x, i) = K e^{-r_i \tau} \mathcal{N}\left(\frac{x_{\min} - x - \mu_i^J}{\sigma_i^J}\right) - K e^{x - q_i \tau + \mu_i^J + \frac{(\sigma_i^J)^2}{2}} \mathcal{N}\left(\frac{x_{\min} - x - \mu_i^J - (\sigma_i^J)^2}{\sigma_i^J}\right)$$

where $\mathcal{N}(\cdot)$ is the cumulative normal distribution, and for Kou model we have

$$R(\tau, x, i) = K(1 - p)\left(e^{-r_i \tau + \eta_2 (x_{\min} - x)} - \frac{\eta_2}{\eta_2 + 1} e^{-\eta_2 x - q_i \tau + (\eta_2 + 1) x_{\min}}\right).$$

For American put option we can calculate $R(\tau, x, i)$ by

$$R(\tau, x, i) = \int_{-\infty}^{x_{\min}} (K - K e^{y}) f(y - x, i) dy,$$

where for Merton model we have

$$R(\tau,x,i)=K\mathcal{N}(\frac{x_{\min}-x-\mu_i^J}{\sigma_i^J})-Ke^{x+\mu_i^J+\frac{(\sigma_i^J)^2}{2}}\mathcal{N}\left(\frac{x_{\min}-x-\mu_i^J-(\sigma_i^J)^2}{\sigma_i^J}\right)$$

and for Kou model we have

$$R(\tau,x,i)=K(1-p)\left(e^{\eta_2(x_{\min}-x)}-\frac{\eta_2}{\eta_2+1}e^{-\eta_2 x+(\eta_2+1)x_{\min}}\right).$$

For approximating $\int_\Omega u(\tau,y,i)f(y-x)dy$ we use the classical numerical integration method known as trapezoidal rule by

$$\int_\Omega u(\tau,y,i)f(y-x,i)dy\approx\frac{h}{2}\left(\sum_{j=0}^{N_x}\omega_j u(\tau,y_j,i)f(y_j-x,i)\right)$$

where $y_j=x_{\min}+jh$ with $h=\frac{x_{\max}-x_{\min}}{N_x}$ where N_x is the number of grids in x direction, and $\omega_j=1$ for $j=0,N_x$ and $\omega_j=2$ for $j=2,...,N_x-1$.

4.3. Fully discretized system

Let $X=\{x_0,x_1,\dots,x_{N_x}\}$ be a set of distinct interpolation points of $[x_{\min},x_{\max}]$, and $\mathcal{T}=\{\tau_0=0<\tau_1<\cdots<\tau_M=T\}$ be a partition of $[0,T]$. Applying the RBF-FD method and the discretization of the integral operator as described in the previous subsections to the time semi-discrete problem (17)–(18), the evaluation of an European option price is reduced to finding an approximation $\mathbf{U}^k:=[\mathbf{U}_1^k,\mathbf{U}_2^k,\cdots,\mathbf{U}_m^k]^\top$ where $\mathbf{U}_i^k=[u(\tau_k,x_1,i),u(\tau_k,x_2,i),\cdots,u(\tau_k,x_{N_x-1},i)]^\top$, as a solution to the following time stepping scheme

$$\frac{\mathbf{U}^1-\mathbf{U}^0}{\triangle\tau}=\mathbf{D}\mathbf{U}^1+\boldsymbol{\lambda}\mathbf{J}\mathbf{U}^0+\overline{\mathbf{Q}}\mathbf{U}^1, \tag{32}$$

$$\frac{\mathbf{U}^{k+1}-\mathbf{U}^{k-1}}{2\triangle\tau}=\mathbf{D}(\frac{\mathbf{U}^{k+1}+\mathbf{U}^{k-1}}{2})+\boldsymbol{\lambda}\mathbf{J}\mathbf{U}^k+\overline{\mathbf{Q}}(\frac{\mathbf{U}^{k+1}+\mathbf{U}^{k-1}}{2}),\quad 1\le k\le M-1, \tag{33}$$

where the initial vector $\mathbf{g}=\mathbf{U}^0=[\mathbf{U}_1^0,\mathbf{U}_2^0,\cdots,\mathbf{U}_m^0]^\top$ defined by $\mathbf{U}_i^0=[g(Ke^{x_1}),g(Ke^{x_2}),\cdots,g(Ke^{x_{N_x-1}})]^\top$ where $g(\cdot)$ is the payoff function (8) and $i\in\mathcal{M}$. One of the sources of error can arise when we use initial function (8) at the RBF-FD grid points, since this function is discontinuous in their first derivatives. A useful notion in the implementation of numerical method is that the value of a function on a grid represents average value of the function over the surrounding grids rather than its value sampled at each grid point [42] by

$$g(x_i)\approx\frac{1}{h}\int_{x_i-\frac{h}{2}}^{x_i+\frac{h}{2}}g(x)dx,$$

and this makes the payoff function smooth at the strike price K, and we use this technique to improve the accuracy of RBF-FD numerical method especially near the strike price. Also, $\mathbf{D}=\text{blkdiag}[\mathbf{D}_1,\mathbf{D}_2,\dots,\mathbf{D}_m]$ where $\mathbf{D}_i$ for $i\in\mathcal{M}$ is the differentiation matrix associated with the differential operator $\mathcal{D}_i$ which will be defined in section 5 and blkdiag means block diagonal, and $\mathbf{J}$ is the integral matrix corresponding to the integral operator defined by $\mathbf{J}=\text{blkdiag}[\mathbf{J}_1,\mathbf{J}_2,\dots,\mathbf{J}_m]$ and $\mathbf{J}_i$ for $i\in\mathcal{M}$ is the integral matrix associated with the discretization of integral operator $\mathcal{J}_i$, $\boldsymbol{\lambda}=\text{blkdiag}[\lambda_1,\lambda_2,\dots,\lambda_m]$, and matrices $\boldsymbol{\lambda}\mathbf{J}=\boldsymbol{\lambda}\otimes\mathbf{J}$ and $\overline{\mathbf{Q}}=\mathbf{Q}\otimes\mathbf{I}_{(N_x-1)\times(N_x-1)}$ where $\otimes$ means tensor product.

For evaluation of an American option price, $\mathbf{U}^k:=[\mathbf{U}_1^k,\mathbf{U}_2^k,\cdots,\mathbf{U}_m^k]^\top$ where $\mathbf{U}_i^k=[u(\tau_k,x_1,i),u(\tau_k,x_2,i),\cdots,u(\tau_k,x_{N_x-1},i)]^\top$ is derived as a solution to the following time stepping schemes

$$\begin{cases}\frac{\widetilde{\mathbf{U}}^1-\mathbf{U}^0}{\triangle\tau}-\mathbf{D}\widetilde{\mathbf{U}}^1-\boldsymbol{\lambda}\mathbf{J}\mathbf{U}^0-\overline{\mathbf{Q}}\widetilde{\mathbf{U}}^1=\boldsymbol{\Upsilon}^0,\\ \boldsymbol{\Upsilon}^1=\boldsymbol{\Upsilon}^0+\frac{\mathbf{U}^1-\widetilde{\mathbf{U}}^1}{\triangle\tau},\\ \boldsymbol{\Upsilon}^1\ge 0,\quad \mathbf{U}^1\ge\mathbf{g},\quad(\boldsymbol{\Upsilon}^1)^\top(\mathbf{U}^1-\mathbf{g})=0,\end{cases} \tag{34}$$

$$\begin{cases}\frac{\widetilde{\mathbf{U}}^{k+1}-\mathbf{U}^{k-1}}{2\triangle\tau}-\mathbf{D}(\frac{\widetilde{\mathbf{U}}^{k+1}+\mathbf{U}^{k-1}}{2})-\boldsymbol{\lambda}\mathbf{J}\mathbf{U}^k-\overline{\mathbf{Q}}(\frac{\widetilde{\mathbf{U}}^{k+1}+\mathbf{U}^{k-1}}{2})=\boldsymbol{\Upsilon}^k,\\ \boldsymbol{\Upsilon}^{k+1}=\boldsymbol{\Upsilon}^k+\frac{\mathbf{U}^{k+1}-\widetilde{\mathbf{U}}^{k+1}}{2\triangle\tau},\\ \boldsymbol{\Upsilon}^{k+1}\ge 0,\quad \mathbf{U}^{k+1}\ge\mathbf{g},\quad(\boldsymbol{\Upsilon}^{k+1})^\top(\mathbf{U}^{k+1}-\mathbf{g})=0,\end{cases} \tag{35}$$

where $\widetilde{\mathbf{U}}^{k+1}$ is an intermediate solution, $\boldsymbol{\Upsilon}^k := [\boldsymbol{\Upsilon}_1^k, \boldsymbol{\Upsilon}_2^k, \cdots, \boldsymbol{\Upsilon}_m^k]^\top$ where $\boldsymbol{\Upsilon}_i^k = [\Upsilon(\tau_k, x_1, i), \Upsilon(\tau_k, x_2, i), \cdots, \Upsilon(\tau_k, x_{N_x-1}, i)]^\top$ is the auxiliary function $\Upsilon(\tau, x, i)$ evaluated at the discretization points.

Each time step is split into two parts. Starting from the initial vector $\mathbf{U}^0 = \mathbf{g}$ and $\boldsymbol{\Upsilon}^0 = \mathbf{0}$, first, the intermediate solution vector $\widetilde{\mathbf{U}}^{k+1}$ is solved from the modified system of linear equations

$$\frac{\widetilde{\mathbf{U}}^{k+1} - \mathbf{U}^{k-1}}{2\triangle\tau} - \mathbf{D}\left(\frac{\widetilde{\mathbf{U}}^{k+1} + \mathbf{U}^{k-1}}{2}\right) - \boldsymbol{\lambda}\mathbf{J}\mathbf{U}^k - \overline{\mathbf{Q}}\left(\frac{\widetilde{\mathbf{U}}^{k+1} + \mathbf{U}^{k-1}}{2}\right) = \boldsymbol{\Upsilon}^k.$$

Second, the intermediate solution $\widetilde{\mathbf{U}}^{k+1}$ is projected to be feasible, and $\boldsymbol{\Upsilon}^k$ is updated in

$$\boldsymbol{\Upsilon}^{k+1} = \boldsymbol{\Upsilon}^k + \frac{\mathbf{U}^{k+1} - \widetilde{\mathbf{U}}^{k+1}}{2\triangle\tau},$$

to satisfy relations

$$\boldsymbol{\Upsilon}^{k+1} \geq 0, \quad \mathbf{U}^{k+1} \geq \mathbf{g}, \quad (\boldsymbol{\Upsilon}^{k+1})^\top(\mathbf{U}^{k+1} - \mathbf{g}) = 0.$$

The update step can be performed very fast and at each spatial grid point independently with the formulas $\mathbf{U}^{k+1} = \max(\mathbf{g}, \widetilde{\mathbf{U}}^{k+1} - 2\triangle\tau\boldsymbol{\Upsilon}^k)$ and $\boldsymbol{\Upsilon}^{k+1} = \boldsymbol{\Upsilon}^k + \frac{\mathbf{U}^{k+1} - \widetilde{\mathbf{U}}^{k+1}}{2\triangle\tau}$.

5. Convergence analysis

In this section, we discuss about consistency and convergence analysis of fully discretized system of equations (32) and (33) with initial condition (8) and boundary condition (14), also we assume that the computed solution belongs to C^∞. To apply RBF-FD discretization for operator $\mathcal{D}_i$ corresponding to the ith regime defined by (9), we show how we can derive the exact RBF-FD formulas for first and second derivatives. In the following, we use multiquadrics as RBFs, defined by

$$\phi(\|\mathbf{x} - \mathbf{y}\|) = \sqrt{\epsilon^2 + (\|\mathbf{x} - \mathbf{y}\|)^2}, \tag{36}$$

where $\|\cdot\|$ is the Euclidean norm and ϵ is the shape parameter. Also, we assume that the grid points in x direction are equidistance with step size h and $n = 3$ is the number of grids in influence domain which are closest neighboring interpolation points to x_j. So, the first derivative of $u(\tau, x, i)$ at $x = x_j$ is approximated by

$$\frac{\partial u}{\partial x}(\tau, x_j, i) = \alpha_{j-1}u(\tau, x_j - h, i) + \alpha_j u(\tau, x_j, i) + \alpha_{j+1}u(\tau, x_j + h, i), \tag{37}$$

so, by substituting function $u(\tau, x, i)$ by multiquadrics radial basis functions centered at $x_j - h, x_j$, and $x_j + h$, the unknown coefficients α_{j-1}, α_j and α_{j+1} are derived by solving a 3×3 linear system of equations, then we have

$$\alpha_{j-1} = -\alpha_{j+1} = -\frac{1}{4h}\frac{1 + \sqrt{1 + \frac{4h^2}{\epsilon^2}}}{\sqrt{1 + \frac{h^2}{\epsilon^2}}}, \quad \alpha_j = 0. \tag{38}$$

In the numerical experiments, we assume $\epsilon \gg h$, so we get [8]

$$\alpha_{j-1} = -\alpha_{j+1} = -\frac{1}{2h}\left(1 + \frac{h^2}{2\epsilon^2}\right), \quad \alpha_j = 0, \tag{39}$$

and since our grid points are equidistance, so for all j, we let

$$\alpha = \alpha_{j+1} = \frac{1}{2h}\left(1 + \frac{h^2}{2\epsilon^2}\right), \quad \alpha_{j-1} = -\alpha, \quad \alpha_j = 0. \tag{40}$$

Now, for second derivative of $u(\tau, x, i)$ at $x = x_j$ let

$$\frac{\partial^2 u}{\partial x^2}(\tau, x_j, i) = \beta_{j-1}u(\tau, x_j - h, i) + \beta_j u(\tau, x_j, i) + \beta_{j+1}u(\tau, x_j + h, i), \tag{41}$$

so, the unknown coefficients β_{j-1}, β_j and β_{j+1} are derived by

$$\beta_{j-1} = \beta_{j+1} = \frac{2 + (\frac{h^2}{\epsilon^2} + 2)\sqrt{1 + \frac{4h^2}{\epsilon^2}} + \frac{5h^2}{\epsilon^2} + \frac{2h^4}{\epsilon^4}}{4h^2(1 + \frac{h^2}{\epsilon^2})^{\frac{3}{2}}}, \quad \beta_j = -\frac{2 + (\frac{h^2}{\epsilon^2} + 2)\sqrt{1 + \frac{4h^2}{\epsilon^2}} + \frac{3h^2}{\epsilon^2}}{2h^2(1 + \frac{h^2}{\epsilon^2})}. \tag{42}$$

Also, if we assume $\epsilon \gg h$, and the gride points are equidistance, then we have [8]

$$\beta_2 = \beta_{j-1} = \beta_{j+1} = \frac{1}{h^2}(1 + \frac{h^2}{\epsilon^2}), \quad \beta_1 = \beta_j = -\frac{2}{h^2}(1 + \frac{h^2}{\epsilon^2}). \tag{43}$$

Now, by substituting the above first and second derivative approximations in operator $\mathcal{D}_i$ we get the following differential matrix

$$\mathbf{D}_i = \frac{1}{2}\sigma_i^2 \begin{pmatrix} \beta_1 & \beta_2 & & & \\ \beta_2 & \beta_1 & \beta_2 & & \\ & \ddots & \ddots & \ddots & \\ & & \beta_2 & \beta_1 & \beta_2 \\ & & & \beta_2 & \beta_1 \end{pmatrix} + (r_i - q_i - \frac{\sigma_i^2}{2} - \lambda_i\kappa_i) \begin{pmatrix} 0 & \alpha & & & \\ -\alpha & 0 & \alpha & & \\ & \ddots & \ddots & \ddots & \\ & & -\alpha & 0 & \alpha \\ & & & -\alpha & 0 \end{pmatrix} - (r_i + \lambda_i)I, \tag{44}$$

finally,

$$\mathbf{D}_i = tridiag\left(\frac{1}{2}\sigma_i^2\beta_2 - (r_i - q_i - \frac{\sigma_i^2}{2} - \lambda_i\kappa_i)\alpha\ ,\ \frac{1}{2}\sigma_i^2\beta_1 - r_i - \lambda_i\ ,\ \frac{1}{2}\sigma_i^2\beta_2 + (r_i - q_i - \frac{\sigma_i^2}{2} - \lambda_i\kappa_i)\alpha\right), \tag{45}$$

where *tridiag* means tridiagonal matrix.

Theorem 1. *Matrix $-\boldsymbol{D}_i$ is a diagonal dominant matrix, if*

$$\frac{2|r_i - q_i - \frac{\sigma_i^2}{2} - \lambda_i\kappa_i|}{\sigma_i^2} < \frac{\beta_2}{\alpha} \approx O(\frac{1}{h}). \tag{46}$$

Proof. Since r_i, λ_i and σ_i are positive for all $i \in \mathcal{M}$ and β_1 is negative, so $r_i + \lambda_i - \frac{1}{2}\sigma_i^2\beta_1 > 0$ which are the diagonal entries of matrix $-\mathbf{D}$. So, for diagonal dominant, we should show that

$$-\frac{1}{2}\sigma_i^2\beta_1 + r_i + \lambda_i > \left|\frac{1}{2}\sigma_i^2\beta_2 - (r_i - q_i - \frac{\sigma_i^2}{2} - \lambda_i\kappa_i)\alpha\right| + \left|\frac{1}{2}\sigma_i^2\beta_2 + (r_i - q_i - \frac{\sigma_i^2}{2} - \lambda_i\kappa_i)\alpha\right|.$$

Now, we consider two cases. First, assume that $(r_i - q_i - \frac{\sigma_i^2}{2} - \lambda_i\kappa_i) \geq 0$, so from (46), we get $\frac{1}{2}\sigma_i^2\beta_2 - (r_i - q_i - \frac{\sigma_i^2}{2} - \lambda_i\kappa_i)\alpha > 0$ and we know $\frac{1}{2}\sigma_i^2\beta_2 + (r_i - q_i - \frac{\sigma_i^2}{2} - \lambda_i\kappa_i)\alpha$ is positive, so

$$\begin{aligned} \left|\frac{1}{2}\sigma_i^2\beta_2 - (r_i - q_i - \frac{\sigma_i^2}{2} - \lambda_i\kappa_i)\alpha\right| + \left|\frac{1}{2}\sigma_i^2\beta_2 + (r_i - q_i - \frac{\sigma_i^2}{2} - \lambda_i\kappa_i)\alpha\right| &= \sigma_i^2\beta_2 \\ &= -\frac{1}{2}\sigma_i^2\beta_1 \\ &< -\frac{1}{2}\sigma_i^2\beta_1 + r_i + \lambda_i \end{aligned} \tag{47}$$

and (47) confirms that matrix $-\mathbf{D}_i$ is a diagonal dominant matrix.

Second, assume that $(r_i - q_i - \frac{\sigma_i^2}{2} - \lambda_i\kappa_i) < 0$, so from (46), we get $\frac{1}{2}\sigma_i^2\beta_2 + (r_i - q_i - \frac{\sigma_i^2}{2} - \lambda_i\kappa_i)\alpha > 0$ and also, we know $\frac{1}{2}\sigma_i^2\beta_2 - (r_i - q_i - \frac{\sigma_i^2}{2} - \lambda_i\kappa_i)\alpha$ is positive, so

$$\begin{aligned} \left|\frac{1}{2}\sigma_i^2\beta_2 - (r_i - q_i - \frac{\sigma_i^2}{2} - \lambda_i\kappa_i)\alpha\right| + \left|\frac{1}{2}\sigma_i^2\beta_2 + (r_i - q_i - \frac{\sigma_i^2}{2} - \lambda_i\kappa_i)\alpha\right| &= \sigma_i^2\beta_2 \\ &= -\frac{1}{2}\sigma_i^2\beta_1 \\ &< -\frac{1}{2}\sigma_i^2\beta_1 + r_i + \lambda_i \end{aligned} \tag{48}$$

and (48) confirms that matrix $-\mathbf{D}_i$ is a diagonal dominant matrix. □

Remark 1. Let $\mathbf{Q}$ as a generated matrix defined by (1), it is easy to derive that matrix $-\mathbf{Q}$ is diagonal dominant with positive diagonal entries, and nonpositive off-diagonal entries.

Theorem 2. *Let $u(\tau, x, i) \in C^{\infty}((0, T] \times [x_{\min}, x_{\max}] \times \mathcal{M})$ satisfies the initial condition (8) and boundary conditions (14) and asymptotic behavior (12). For sufficiently small h and $\triangle\tau$ and all $i \in \mathcal{M}$,*

$$\frac{\partial u(\tau_k, x_j, i)}{\partial \tau} - \mathcal{L}_i u(\tau_k, x_j, i) = \frac{u(\tau_{k+1}, x_j, i) - u(\tau_{k-1}, x_j, i)}{2\triangle\tau} - \mathbf{L}_i u(\tau_k, x_j, i) + O((\triangle\tau)^2 + h^2 + \frac{h^2}{\epsilon^2}), \tag{49}$$

where

$$\mathcal{L}_i u(\tau, x, i) = \mathcal{D}_i u(\tau, x, i) + \lambda_i \mathcal{J}_i u(\tau, x, i) + \sum_{j=1}^{m} q_{ij} u(\tau, x, i),$$

and $\mathbf{L}_i$ is the corresponding discretized operator to the $\mathcal{L}_i$.

Proof. By using the RBF-FD approximation for first and second derivatives of differential operator $\mathcal{D}_i$ defined by (9), so we have

$$\frac{\partial u(\tau_k, x_j, i)}{\partial x} - [\frac{u(\tau_k, x_{j+1}, i) - u(\tau_k, x_{j-1}, i)}{2h}](1 + \frac{h^2}{2\epsilon^2}) \approx \frac{h^2}{6}\frac{\partial^3 u(\tau_k, x_j, i)}{\partial x^3} + \frac{h^2}{2\epsilon^2}\frac{\partial u(\tau_k, x_j, i)}{\partial x} \tag{50}$$

so,

$$\begin{aligned}\frac{\partial u(\tau_k, x_j, i)}{\partial x} = \frac{1}{2}[&\frac{u(\tau_{k+1}, x_{j+1}, i) - u(\tau_{k+1}, x_{j-1}, i)}{2h} \\ &+ \frac{u(\tau_{k-1}, x_{j+1}, i) - u(\tau_{k-1}, x_{j-1}, i)}{2h}](1 + \frac{h^2}{2\epsilon^2}) + O((\triangle\tau)^2 + h^2 + \frac{h^2}{\epsilon^2}),\end{aligned} \tag{51}$$

and for second derivative

$$\begin{aligned}&\frac{\partial^2 u(\tau_k, x_j, i)}{\partial x^2} - [\frac{u(\tau_k, x_{j+1}, i) - 2u(\tau_k, x_j, i) + u(\tau_k, x_{j-1}, i)}{h^2}](1 + \frac{h^2}{\epsilon^2}) \\ &\quad\approx \frac{h^2}{12}\frac{\partial^4 u(\tau_k, x_j, i)}{\partial x^4} + \frac{h^2}{\epsilon^2}\frac{\partial^2 u(\tau_k, x_j, i)}{\partial x^2} - \frac{3h^2}{4\epsilon^2}u(\tau_k, x_j, i)\end{aligned}$$

then

$$\begin{aligned}\frac{\partial^2 u(\tau_k, x_j, i)}{\partial x^2} = \frac{1}{2}[&\frac{u(\tau_{k+1}, x_{j+1}, i) - 2u(\tau_{k+1}, x_j, i) + u(\tau_{k+1}, x_{j-1}, i)}{h^2} \\ &+ \frac{u(\tau_{k-1}, x_{j+1}, i) - 2u(\tau_{k-1}, x_j, i) + u(\tau_{k-1}, x_{j-1}, i)}{h^2}](1 + \frac{h^2}{\epsilon^2}) + O((\triangle\tau)^2 + h^2 + \frac{h^2}{\epsilon^2})\end{aligned} \tag{52}$$

by using the first derivative approximation (51) and second derivative approximation (52) the differential operator $\mathcal{D}_i$ is approximated by the discrete operator $\mathbf{D}_i$ with the error at each grid point (τ_k, x_j, i)

$$\mathcal{D}_i u(\tau_k, x_j, i) = \mathbf{D}_i(\frac{u(\tau_{k+1}, x_j, i) + u(\tau_{k-1}, x_j, i)}{2}) + O((\triangle\tau)^2 + h^2 + \frac{h^2}{\epsilon^2}). \tag{53}$$

For the integral operator we have

$$\int_{\mathbb{R}} u(\tau_k, y, i) f(y - x_j, i) dy = \frac{h}{2}\left(\sum_{v=1}^{N_x} \omega_v u(\tau_k, y_v, i) f(y_v - x_j, i)\right) + R(\tau_k, x_j, i) + O(h^2)$$

therefore

$$\mathcal{J}_i u(\tau_k, x_j, i) = \mathbf{J}_i u(\tau_k, x_j, i) + O(h^2). \tag{54}$$

In addition, we need the following interpolation error

$$\left|\sum_{j=1}^{m} q_{ij} u(\tau_k, x_j, i) - \sum_{j=1}^{m} q_{ij}\frac{u(\tau_{k+1}, x_j, i) + u(\tau_{k-1}, x_j, i)}{2}\right| \le \frac{(\triangle\tau)^2}{2}\sup_{\tau\in[\tau_{k-1}, \tau_{k+1}]}\left|\frac{\partial^2 u}{\partial \tau^2}(\tau, x_j, i)\right| \tag{55}$$

Now, let

$$\mathcal{L}_i u(\tau, x, i) = \mathcal{D}_i u(\tau, x, i) + \lambda_i \mathcal{J}_i u(\tau, x, i) + \sum_{j=1}^{m} q_{ij} u(\tau, x, i),$$

then by using (53) for differential operator approximation, (54) for integral operator approximation and (55) for identity part, we get

$$\mathcal{L}_i u(\tau_k, x_j, i) = \mathbf{L}_i u(\tau_k, x_j, i) + O((\triangle\tau)^2 + h^2 + \frac{h^2}{\epsilon^2}). \tag{56}$$

Also, for the time derivative we have the following approximation

$$\frac{\partial u(\tau_k, x_j, i)}{\partial \tau} = \frac{u(\tau_{k+1}, x_j, i) - u(\tau_{k-1}, x_j, i)}{2\triangle\tau} + O((\triangle\tau)^2), \tag{57}$$

so, finally by using (56) and (57), we get

$$\frac{\partial u(\tau_k, x_j, i)}{\partial \tau} - \mathcal{L}_i u(\tau_k, x_j, i) = \frac{u(\tau_{k+1}, x_j, i) - u(\tau_{k-1}, x_j, i)}{2\triangle\tau} - \mathbf{L}_i u(\tau_k, x_j, i) + O((\triangle\tau)^2 + h^2 + \frac{h^2}{\epsilon^2}),$$

and this completes the proof. □

Let us define the error vector $\mathbf{E}^k = [\mathbf{u}_1^k - \mathbf{U}_1^k, \mathbf{u}_2^k - \mathbf{U}_2^k, \ldots, \mathbf{u}_m^k - \mathbf{U}_m^k]^T$ where $\mathbf{u}_i^k$ is the exact solution of (7) with initial condition (8) and boundary condition (12) for ith regime and kth time level, and $\mathbf{U}_i^k$ is the solution derived by solving linear system of equations (33). Also, let $\bar{\mathbf{I}} = \mathbf{I}_{m\times m} \otimes \mathbf{I}_{(N_x-1)\times(N_x-1)}$, $\overline{\mathbf{Q}} = \mathbf{Q} \otimes \mathbf{I}_{(N_x-1)\times(N_x-1)}$ and $\mathbf{d}$ is the column vector of size $m \times (N_x - 1)$ with entries $\triangle\tau\, O((\triangle\tau)^2 + h^2 + \frac{h^2}{\epsilon^2})$. Now, by using (33) and (49), we obtain the error vector by solving the following system of equations

$$(\bar{\mathbf{I}} - \triangle\tau(\overline{\mathbf{Q}} + \mathbf{D}))\mathbf{E}^{k+1} = (\bar{\mathbf{I}} + \triangle\tau(\overline{\mathbf{Q}} + \mathbf{D}))\mathbf{E}^{k-1} + 2\triangle\tau\boldsymbol{\lambda}\mathbf{J}\mathbf{E}^k + \mathbf{d}. \tag{58}$$

Lemma 1. *If $\mathbf{A} := (a_{ij})$ is a diagonal dominant matrix, then for any vector $\mathbf{x}$ the inequality*

$$\|\mathbf{x}\|_\infty \le \|(\mathbf{I} + \triangle\tau\mathbf{A})\mathbf{x}\|_\infty, \tag{59}$$

is satisfied, and also, if $\triangle\tau \le \frac{1}{\max_i |a_{ii}|}$, then $\|(\mathbf{I} - \triangle\tau\mathbf{A})\mathbf{x}\|_\infty \le 1$.

Proof. [30] □

Lemma 2. *Let $\{a_n\}_{n\ge 0}$ be a nonnegative sequence such that for $n \ge 2$*

$$a_n \le a_{n-2} + K'\triangle\tau a_{n-1} + d,$$

where three terms K', $\triangle\tau$ and d are positive constants. If $a_0 = 0$ then for $n \ge 2$

$$a_n \le (1 + K'\triangle\tau)^{n-1}a_1 + d\sum_{j=0}^{n-2}(1 + K'\triangle\tau)^j.$$

Proof. [35] □

Theorem 3. *Let $u(\tau, x, i)$ is the solution of the PIDE (7) with initial condition (8) and boundary condition (14), and let $\mathbf{U}_i^k$ is the solution derived by solving linear system of equations (33). If h and $\triangle\tau$ are sufficiently small, then for system of equations defined by (58) we have*

$$\|\mathbf{E}^{k+1}\|_\infty \le e^{2\lambda T}\triangle\tau\, O(\triangle\tau + h^2 + \frac{h^2}{\epsilon^2}) + \frac{e^{2\lambda T} - 1}{2\lambda} O((\triangle\tau)^2 + h^2 + \frac{h^2}{\epsilon^2}), \tag{60}$$

where $\lambda = \max\lambda_i$ for $i \in \mathcal{M}$ and λ_i is the i-th intensity rate and T is time of maturity.

Proof. From Theorem 1 and Remark 1, matrix $-(\overline{\mathbf{Q}} + \mathbf{D})$ is a diagonal dominant matrix and let $\mathbf{A} = -(\overline{\mathbf{Q}} + \mathbf{D})$ in Lemma 1, so we get

$$\begin{aligned}\|\mathbf{E}^{k+1}\|_\infty &\le \|(\bar{\mathbf{I}} - \triangle\tau(\overline{\mathbf{Q}} + \mathbf{D}))\mathbf{E}^{k+1}\|_\infty \\ &\le \|(\bar{\mathbf{I}} + \triangle\tau(\overline{\mathbf{Q}} + \mathbf{D}))\|_\infty\|\mathbf{E}^{k-1}\|_\infty + 2\lambda\triangle\tau\|\mathbf{J}\|_\infty\|\mathbf{E}^k\|_\infty + \|\mathbf{d}\|_\infty,\end{aligned}$$

where $\lambda = \max\lambda_i$. A right stochastic matrix is a square matrix of nonnegative real numbers, with each row summing to one [25]. We assume that $\mathbf{J}$ does not have error due to the truncation of the domain, so matrix $\mathbf{J}$ leads to a non-negative right

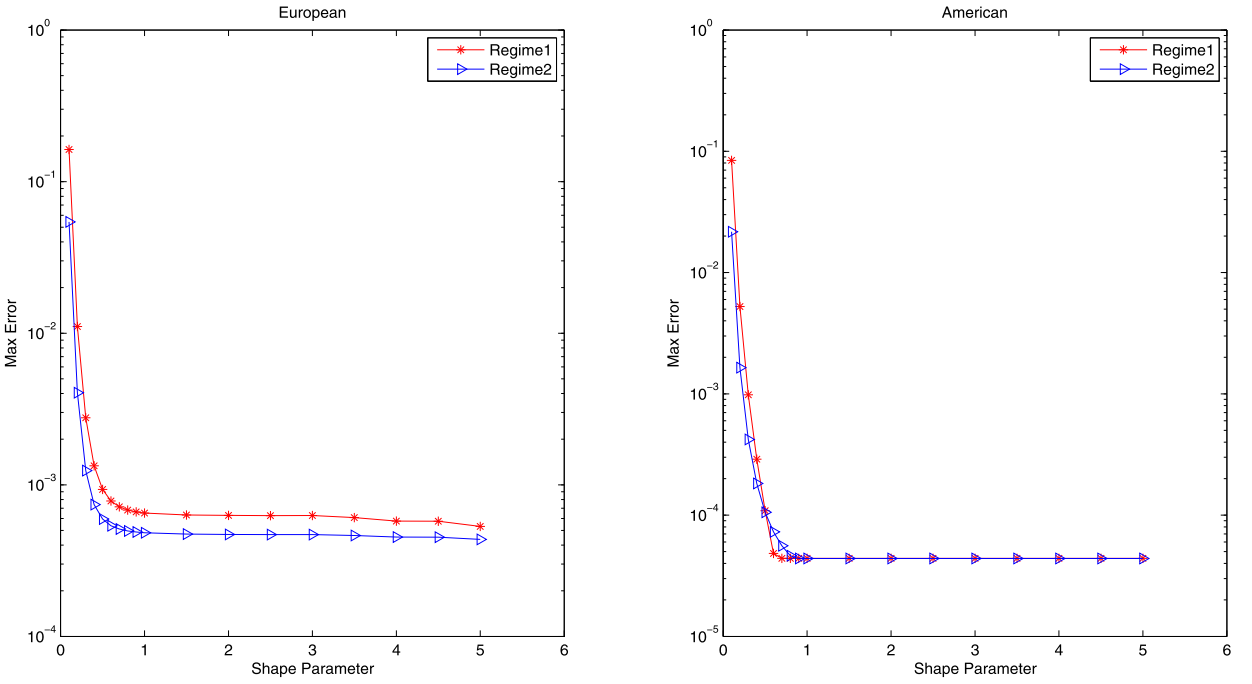

Fig. 1. Maximum error as function of the shape parameter ϵ for European and American options and Example 1.

stochastic matrix [45]. Therefore $\|\mathbf{J}\|_\infty \leq 1$ then

$$\|\mathbf{E}^{k+1}\|_\infty \leq \|\mathbf{E}^{k-1}\|_\infty + 2\lambda\triangle\tau\|\mathbf{J}\|_\infty\|\mathbf{E}^k\|_\infty + \|\mathbf{d}\|_\infty.$$

Now, by using Lemma 2, we have

$$\begin{aligned}\|\mathbf{E}^{k+1}\|_\infty &\leq (1+2\lambda\triangle\tau)^k \max\left\{\|\mathbf{E}^0\|_\infty, \|\mathbf{E}^1\|_\infty\right\} + \|\mathbf{d}\|_\infty \sum_{j=0}^{k-1}(1+2\lambda\triangle\tau)^j \\ &\leq e^{2\lambda T}\max\left\{\|\mathbf{E}^0\|_\infty, \|\mathbf{E}^1\|_\infty\right\} + \frac{e^{2\lambda T}-1}{2\lambda\triangle\tau}\|\mathbf{d}\|_\infty,\end{aligned}$$

and we know that $\|\mathbf{E}^0\|_\infty = 0$, $\|\mathbf{E}^1\|_\infty \leq \triangle\tau\, O(\triangle\tau + h^2 + \frac{h^2}{\epsilon^2})$ and $\|\mathbf{d}\|_\infty \leq \triangle\tau\, O((\triangle\tau)^2 + h^2 + \frac{h^2}{\epsilon^2})$, finally we have

$$\|\mathbf{E}^{k+1}\|_\infty \leq e^{2\lambda T}\triangle\tau\, O(\triangle\tau + h^2 + \frac{h^2}{\epsilon^2}) + \frac{e^{2\lambda T}-1}{2\lambda} O((\triangle\tau)^2 + h^2 + \frac{h^2}{\epsilon^2}). \quad \square$$

6. Numerical results

In this section, we carry out some numerical experiments to evaluate the prices of European and American options under the regime switching model with jump. As RBF for spatial discretization, we select the multiquadric radial basis function defined by (36) with $\epsilon = 1$ for all American and European options, and we choose $n = 3$ as number of local nodes in each stencil, and all experiments are performed on a PC with a 3.6 GHz Corei3 processor.

Figs. 1 and 2 display the dependence of the maximum error on the size of the shape parameter for European and American options for Examples 1 and 3. We derive from these figurers that $\epsilon = 1$ is a good and optimal choice for our numerical experiments.

For a special case presented in Example 1, we will derive a closed form solution, but in general cases, for European and American options, closed form solution is not available, so in tables, Error refers to the difference between successive numerical solutions following mesh refinements at specific grid point S_j, given by

$$\text{Error} = \left|V_{h,\triangle\tau}(0, S_j, i) - V_{\frac{h}{2},\frac{\triangle\tau}{2}}(0, S_j, i)\right|,$$

where $h = \frac{x_{\max}-x_{\min}}{N_x}$ and $\triangle\tau = \frac{T}{M}$ are space and time step sizes, respectively. Also, Ratio denotes the $\log_2$ ratio of errors defined by

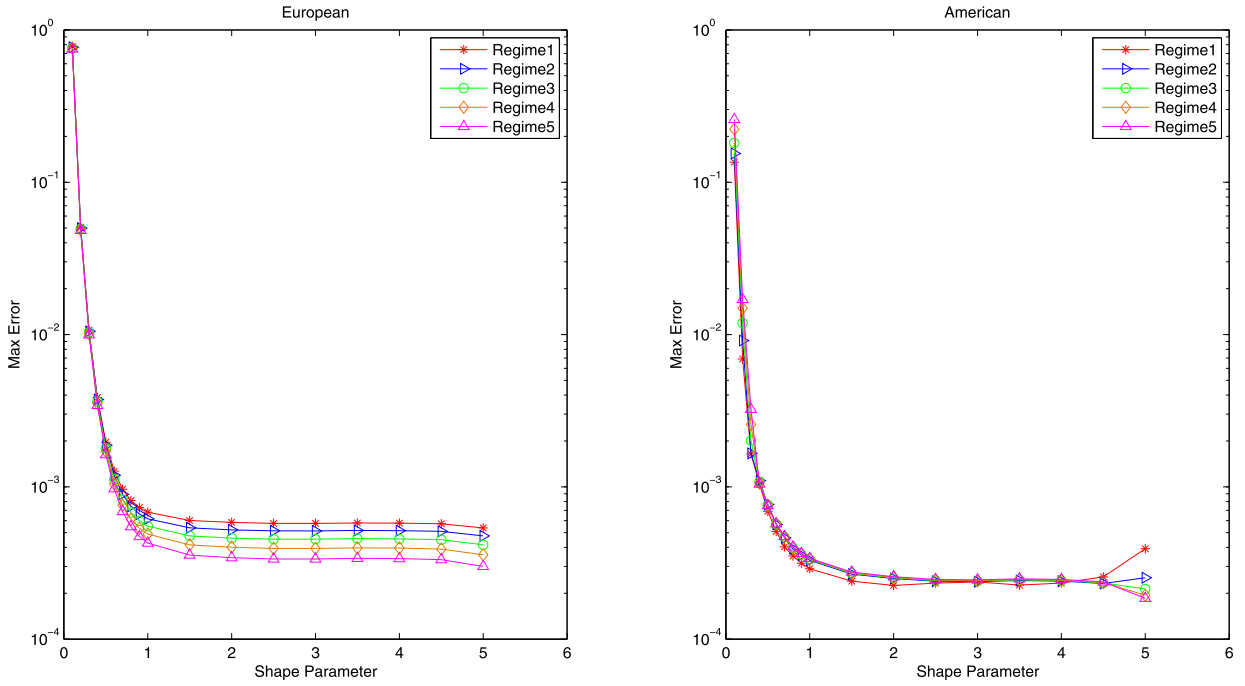

Fig. 2. Maximum error as function of the shape parameter ϵ for European and American options and Example 3.

$$\text{Ratio} = \log_2\left(\left|\frac{V_{h,\triangle\tau}(0,S_j,i) - V_{\frac{h}{2},\frac{\triangle\tau}{2}}(0,S_j,i)}{V_{\frac{h}{2},\frac{\triangle\tau}{2}}(0,S_j,i) - V_{\frac{h}{4},\frac{\triangle\tau}{4}}(0,S_j,i)}\right|\right).$$

Example 1. In this example, we consider European and American put option under the regime switching model with parameters

$$\begin{pmatrix} r_1 \\ r_2 \end{pmatrix} = \begin{pmatrix} 0.08 \\ 0.08 \end{pmatrix}, \quad \begin{pmatrix} \sigma_1 \\ \sigma_2 \end{pmatrix} = \begin{pmatrix} 0.3 \\ 0.1 \end{pmatrix}, \quad \mathbf{Q} = \begin{pmatrix} -0.5 & 0.5 \\ 0.5 & -0.5 \end{pmatrix}, \quad T = 1, \quad K = 40$$

and jump parameters for $i = 1, 2$ are $\mu_i^J = -0.025, \sigma_i^J = \sqrt{0.05}$, $\lambda_i = 5$ and $q_i = 0$ chosen from [15,43].

To derive a closed-form solution for European option, we have to consider a special case where $m = 2$ (two regimes) and the jump process (the Poisson process N and the jump sizes Y) do not depend on the Markov chain α_t, i.e., $Y_{\alpha_t} = Y$, $\lambda_{\alpha_t} = \lambda$, and $\kappa_{\alpha_t} = \kappa$. We also assume that the log jump size $\ln Y$ follows the Merton's normal distribution with mean μ^J and variance $(\sigma^J)^2$. Then we have $S_t = e^{X_t}$, where

$$X_t = X_0 + \int_0^t \left(r_{\alpha_s} - q_{\alpha_s} - \frac{1}{2}\sigma_{\alpha_s}^2 - \lambda\kappa\right) ds + \int_0^t \sigma_{\alpha_s} dW(s) + \sum_{j=1}^{N_t} \ln Y_j,$$

where $X_0 = \ln S_0$.

For convenience, let $a_{\alpha_s} = r_{\alpha_s} - q_{\alpha_s} - \frac{1}{2}\sigma_{\alpha_s}^2 - \lambda\kappa$. Given $\{\alpha_s : 0 \le s \le T\}$ and $N_T = n$. Then X_T is a conditional normal random variable with conditional mean and variance given by

$$E[X_T] = X_0 + \int_0^T a_{\alpha_s} ds + n\mu^J,$$

$$Var[X_T] = \int_0^T \sigma_{\alpha_s}^2 ds + n(\sigma^J)^2.$$

Let

$$T_i = \int_0^T I_{\{\alpha_s = i\}} ds, \quad i = 1, 2,$$

be the sojourn time of the Markov chain α_t in state i during the interval $[0, T]$. Then $T_1 + T_2 = T$. It follows that

$$E[X_T] = X_0 + a_1 T_1 + a_2 (T - T_1) + n\mu^J = X_0 + (a_1 - a_2) T_1 + a_2 T + n\mu^J,$$
$$Var[X_T] = \sigma_1^2 T_1 + \sigma_2^2 (T - T_1) + n(\sigma^J)^2 = (\sigma_1^2 - \sigma_2^2) T_1 + \sigma_2^2 T + n(\sigma^J)^2.$$

The European put option prices $V_1(S)$ and $V_2(S)$ at time $t = 0$ are given by

$$V_i(S) = \tilde{E}\left\{ \exp\left(-\int_0^T r_{\alpha_t}\, dt \right) (K - S_T)^+ \middle| S_0 = S, \alpha_0 = i \right\}$$
$$= \sum_{n=0}^{\infty} e^{-\lambda T} \frac{(\lambda T)^n}{n!} \tilde{E}\left\{ e^{-(r_1 - r_2)T_1 - r_2 T} (K - e^{X_T})^+ \middle| S_0 = S, \alpha_0 = i, N_T = n \right\},$$

where $\tilde{E}(\cdot)$ is the expectation operator. Note that the conditional distribution of X_T depends on the trajectory $\{\alpha_s : 0 \le s \le T\}$ via T_1. Given $T_1 = t$, we have

$$\tilde{E}\left\{ e^{-(r_1 - r_2)T_1 - r_2 T} (K - e^{X_T})^+ \middle| S_0 = S, \alpha_0 = i, N_T = n, T_1 = t \right\}$$
$$= \int_{-\infty}^{\ln K} e^{-(r_1 - r_2)t - r_2 T} (K - e^x) \rho(x, m(t), v(t)) dx$$
$$= \int_0^K e^{-(r_1 - r_2)t - r_2 T} \frac{y}{K - y} \rho\left(\ln(K - y), m(t), v(t)\right) dy$$

where the substitution $y = K - e^x$ was used, and $\rho(x, m(t), v(t))$ is the Gaussian density function with mean $m(t)$ and variance $v(t)$ given by,

$$m(t) = \ln S + (a_1 - a_2)t + a_2 T + n\mu^J,$$
$$v(t) = (\sigma_1^2 - \sigma_2^2)t + \sigma_2^2 T + n(\sigma^J)^2.$$

Finally, we obtain the closed-form solution for $V_1(S)$ and $V_2(S)$ by taking integral with respect to the density function of T_1

$$V_i(S) = \sum_{n=0}^{\infty} e^{-\lambda T} \frac{(\lambda T)^n}{n!} \int_0^K \int_0^T e^{-(r_1 - r_2)t - r_2 T} \frac{y}{K - y} \rho\left(\ln(K - y), m(t), v(t)\right) f_i(t, T)\, dt\, dy\,, \tag{61}$$

where [26]

$$f_1(t, T) = e^{q_{11} T} \delta_0(T - t) + e^{q_{22} T + (q_{11} - q_{22})t}$$
$$\times \left(\sqrt{\frac{q_{11} q_{22} t}{T - t}} I_1(2\sqrt{q_{11} q_{22} t (T - t)}) - q_{11} I_0(2\sqrt{q_{11} q_{22} t (T - t)}) \right)$$
$$f_2(t, T) = e^{q_{22} T} \delta_0(t) + e^{q_{22} T + (q_{11} - q_{22})t}$$
$$\times \left(\sqrt{\frac{q_{11} q_{22} (T - t)}{t}} I_1(2\sqrt{q_{11} q_{22} t (T - t)}) - q_{22} I_0(2\sqrt{q_{11} q_{22} t (T - t)}) \right)$$

where $\delta_0(\cdot)$ is the Dirac Delta function, $I_0(\cdot)$ and $I_1(\cdot)$ are the modified Bessel functions given by

$$I_0(z) = \sum_{n=0}^{\infty} \frac{\left(\frac{z}{2}\right)^{2n}}{(n!)^2}, \quad I_1(z) = \sum_{n=0}^{\infty} \frac{\left(\frac{z}{2}\right)^{2n+1}}{n!(n+1)!}.$$

For the given set of parameters numerical results are reported in Table 1 at $S = K = 40$ for different regimes and European and American options with the truncated domain of the log price $[x_{\min}, x_{\max}] = [-2, 2]$. Also, analytical solutions for European option reported in Table 1 at $S = K = 40$ for different regimes are derived from (61). The parameter set of this example has been considered in [43] and finite element scheme was employed for pricing European option under regime switching jump diffusion processes. Comparing numerical results given in Table 1 of [43] with the results of present paper

Table 1
Numerical results for European and American put options under regime switching of Merton model for Example 1 at $S = K = 40$.

N_x	M	European				American			
		Price	Absolute error	Time (s)	Ratio	Price	Error	Time (s)	Ratio
Regime 1									
50	50	7.0391789	2.2(-3)	0.095		7.3826097		0.115	
100	100	7.0374726	5.6(-4)	0.349	2.012	7.3818215	7.8(-4)	0.402	
200	200	7.0370477	1.3(-4)	0.397	2.031	7.3816092	2.1(-4)	0.493	1.893
400	400	7.0369430	3.2(-5)	0.742	2.064	7.3815324	7.6(-5)	0.903	1.465
800	800	7.0369173	7.2(-6)	2.849	2.183	7.3814998	3.2(-5)	3.004	1.237
1600	1600	7.0369120	2.0(-6)	19.18	1.836	7.3814871	1.2(-5)	20.75	1.365
Analytical solution		7.0369101							
Regime 2									
50	50	6.3183120	2.0(-3)	0.095		6.6289657		0.115	
100	100	6.3167538	5.2(-4)	0.349	1.999	6.6290914	1.2e(4)	0.402	
200	200	6.3163626	1.2(-4)	0.397	2.013	6.6291911	9.9(-5)	0.493	0.335
400	400	6.3162654	3.1(-5)	0.742	2.025	6.6292294	3.8(-5)	0.903	1.378
800	800	6.3162413	7.4(-6)	2.849	2.084	6.6292371	7.6(-6)	3.004	2.319
1600	1600	6.3162357	1.9(-6)	19.18	1.936	6.6292373	2.5(-7)	20.75	4.931
Analytical solution		6.3162338							

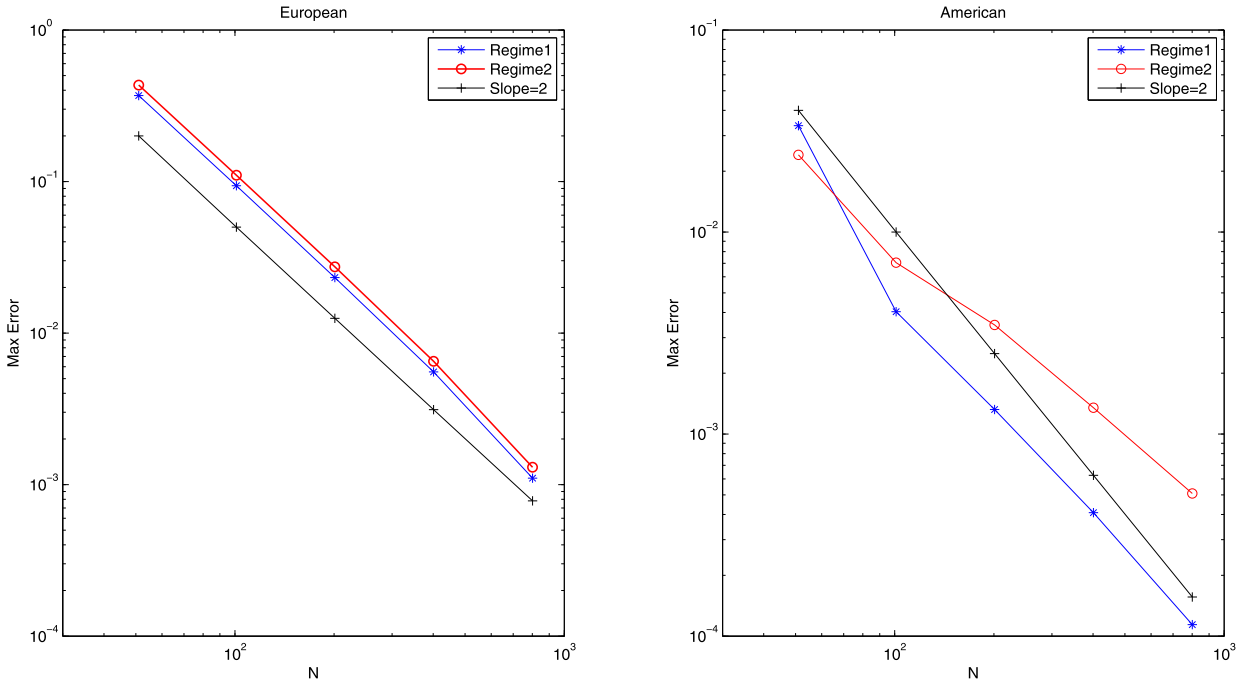

Fig. 3. Left: Error convergence in space for European put option using 1600 time discretization steps. Right: Error convergence in space for American put option using 1600 time discretization steps.

shows that RBF-FD method is accurate than finite element scheme. Also, in [15], the numerical solution for first and second regime are 7.0369 and 6.3177 generated using 2000 time steps and reported in Table 7 of [15], by comparing with the analytical solution given in Table 1, it is easy to derive that RBF-FD method is accurate than multinomial lattice approach presented in [15].

For more investigation about the efficiency of RBF-FD method, we define the following maximum error

$$Max\ Error = \max_j |V(0, S_j, i) - V^{ref}(0, S_j, i)| \tag{62}$$

where $S_j \in [Ke^{-3}, Ke^3]$ corresponding with $x_j \in [x_{\min}, x_{\max}] = [-3, 3]$ and $i = 1, 2$. In the definition of *Max Error*, we use a very accurate solution obtained by the RBF-FD approximation with a very large number of grid points 3200 and time steps 3200 as $V^{ref}(0, S_j, i)$. Fig. 3 depicts the rate of convergence in space for European and American options.

Table 2
Numerical results for European put option under regime switching of Merton model for Example 1 at $S = K = 40$ for large jump intensity values.

N_x	M	$\lambda_i = 25$			$\lambda_i = 50$		
		Price	Absolute error	Ratio	Price	Error	Ratio
Regime 1							
50	50	15.1249770	1.9(-2)		20.5804952	5.2(-2)	
100	100	15.1388321	5.2(-3)	1.867	20.6178556	1.5(-2)	1.770
200	200	15.1427231	1.3(-3)	1.965	20.6293012	4.0(-3)	1.937
400	400	15.1437257	3.3(-4)	1.991	20.6323213	1.0(-3)	1.978
800	800	15.1439782	8.4(-5)	1.997	20.6330889	2.5(-4)	1.985
1600	1600	15.1440413	2.1(-5)	1.981	20.6332819	6.6(-5)	1.966
Analytical solution		15.1440626			20.6333483		
Regime 2							
50	50	14.8368272	1.3(-2)		20.4156739	3.9(-2)	
100	100	14.8467467	3.7(-3)	1.865	20.4432097	1.1(-2)	1.735
200	200	14.8495402	9.6(-4)	1.965	20.4519236	3.1(-3)	1.927
400	400	14.8502598	2.4(-4)	1.991	20.4542423	7.9(-4)	1.976
800	800	14.8504411	6.0(-5)	1.997	20.4548330	1.9(-4)	1.987
1600	1600	14.8504864	1.5(-5)	1.981	20.4549816	5.0(-5)	1.973
Analytical solution		14.8505017			20.4550323		

Table 3
Numerical results for European put option under regime switching of Merton model for Example 1 at $S = K = 40$ with high volatility.

N_x	M	Regime 1			Regime 2		
		Price	Absolute error	Ratio	Price	Error	Ratio
50	50	22.7016107	9.9(-1)		16.7542614	3.0(-1)	
100	100	23.4200793	2.7(-1)	1.860	16.9735597	8.2(-2)	1.872
200	200	23.6229010	7.0(-2)	1.958	17.0348450	2.1(-2)	1.964
400	400	23.6753534	1.7(-2)	1.978	17.0506282	5.3(-3)	1.985
800	800	23.6886438	4.5(-3)	1.971	17.0546134	1.3(-3)	1.983
1600	1600	23.6920002	1.1(-3)	1.930	17.0556124	3.5(-4)	1.946
Analytical solution		23.6931939			17.0559626		

We know that closed form solutions are not available for European options under more than two regimes and jump diffusion process as well as all American options, so for testing the accuracy and efficiency of RBF-FD method and investigating on the rate of convergence, we devote more considerations to this example since analytical solution is available, and we have a possibility to test efficiency of proposed method by changing different type of parameters. Therefore, to study the influence of the large jump intensities λ_i on the convergence rate and accuracy, we consider same parameters except that the jump intensities λ_i for $i = 1, 2$ are replaced by 25 and 50 respectively. The results for European option are reported in Table 2 at $S = K = 40$ for different regimes with the truncated domain of the log price $[x_{\min}, x_{\max}] = [-5, 5]$, and analytical solutions are derived from (61).

To show the efficiency of RBF-FD method, also we report the results for high volatility, so we consider same parameters except that the volatilities σ_i for $i = 1, 2$ are replaced by 2 and 1 respectively. The results for European option are reported in Table 3 at $S = K = 40$ for different regimes with the truncated domain of the log price $[x_{\min}, x_{\max}] = [-5, 5]$, and analytical solutions are derived from (61). Convergence rates for large jump intensity and high volatility are depicted in Fig. 4 and confirms the stability and accuracy of RBF-FD method combined by three time level discretization for European option. Also, for computing maximum error defined by (62) we let $S_j \in [Ke^{-5}, Ke^{5}]$ corresponding with $x_j \in [x_{\min}, x_{\max}] = [-5, 5]$.

Example 2. In this example, we consider European and American put option under the regime switching model with parameters

$$\begin{pmatrix} r_1 \\ r_2 \\ r_3 \end{pmatrix} = \begin{pmatrix} 0.05 \\ 0.05 \\ 0.05 \end{pmatrix}, \quad \begin{pmatrix} \sigma_1 \\ \sigma_2 \\ \sigma_3 \end{pmatrix} = \begin{pmatrix} 0.15 \\ 0.15 \\ 0.15 \end{pmatrix}, \quad \begin{pmatrix} \lambda_1 \\ \lambda_2 \\ \lambda_3 \end{pmatrix} = \begin{pmatrix} 0.3 \\ 0.5 \\ 0.7 \end{pmatrix} \quad \mathbf{Q} = \begin{pmatrix} -0.8 & 0.6 & 0.2 \\ 0.2 & -1 & 0.8 \\ 0.1 & 0.3 & -0.4 \end{pmatrix}.$$

All options have maturity time $T = 1$ and exercise price $K = 100$, and jump parameters for $i = 1, 2, 3$ are $\mu_i^J = -0.5, \sigma_i^J = 0.45$, and $q_i = 0$ chosen from [36,43]. The results are reported in Tables 4 and 5 at $S = 90, 100, 110$ for different regimes and European and American options with the truncated domain of the log price $[x_{\min}, x_{\max}] = [-1.5, 1.5]$.

The prices of the European put option at the first state of the economy under the regime switching Merton model by using the implicit method with three time levels have been presented in Table 1 of [36]. Comparison of the numerical results

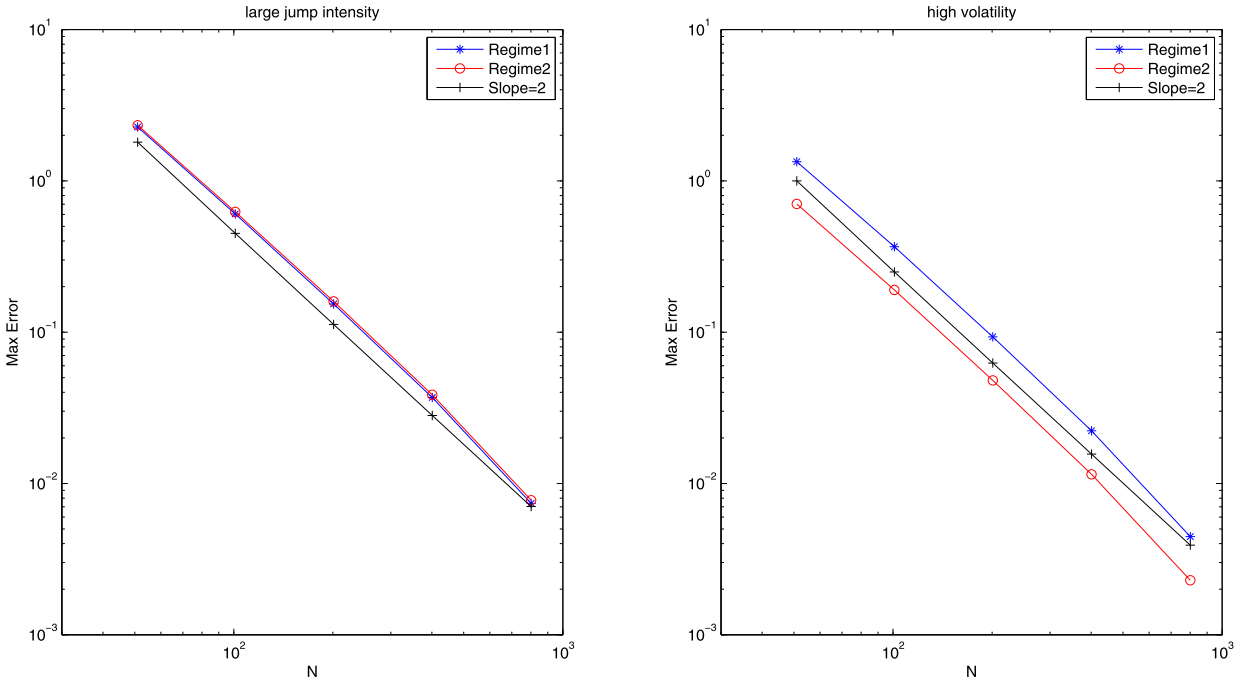

Fig. 4. Left: Error convergence for large jump intensity $\lambda_i = 50$ in space using 1600 time discretization steps for European put option. Right: Error convergence for high volatility in space using 1600 time discretization steps for European put option.

Table 4
Numerical results for European put option under regime switching of Merton model for Example 2.

N_x	M	$S = 90$			$S = 100$			$S = 110$			Time (s)
		Price	Error	Ratio	Price	Error	Ratio	Price	Error	Ratio	
Regime 1											
50	50	13.497753			10.498988			8.725180			0.099
100	100	13.520459	2.2(-2)		10.534547	3.5(-2)		8.743977	1.8(-2)		0.127
200	200	13.526355	5.8(-2)	1.945	10.543064	8.5(-2)	2.062	8.748600	4.6(-3)	2.024	0.308
400	400	13.527850	1.4(-3)	1.980	10.545179	2.1(-3)	2.010	8.749756	1.1(-3)	1.999	0.900
800	800	13.528229	3.7(-4)	1.980	10.545710	5.3(-4)	1.994	8.750048	2.9(-4)	1.988	4.195
1600	1600	13.528330	1.0(-4)	1.896	10.545847	1.3(-4)	1.945	8.750123	7.5(-5)	1.947	38.403
Regime 2											
50	50	15.723340			13.057382			11.228812			0.099
100	100	15.767713	4.4(-2)		13.094860	3.7(-2)		11.244196	1.5(-2)		0.127
200	200	15.778620	1.0(-2)	2.024	13.103741	8.8(-3)	2.077	11.248042	3.8(-3)	2.000	0.308
400	400	15.781342	2.7(-3)	2.002	13.105943	2.2(-3)	2.012	11.249009	9.6(-4)	1.991	0.900
800	800	15.782028	6.8(-4)	1.990	13.106496	5.5(-4)	1.992	11.249254	2.4(-4)	1.979	4.195
1600	1600	15.782205	1.7(-4)	1.951	13.106638	4.2(-5)	1.961	11.249318	6.4(-5)	1.938	38.403
Regime 3											
50	50	17.427609			14.868918			12.939276			0.099
100	100	17.481211	5.3(-2)		14.901355	3.2(-2)		12.950619	1.1(-2)		0.127
200	200	17.493948	1.2(-2)	2.073	14.909056	7.7(-3)	2.074	12.953575	2.9(-3)	1.940	0.308
400	400	17.497104	3.1(-3)	2.013	14.910970	1.9(-3)	2.009	12.954327	7.5(-4)	1.974	0.900
800	800	17.497896	7.9(-4)	1.995	14.911451	4.8(-4)	1.991	12.954519	1.9(-4)	1.972	4.195
1600	1600	17.498099	2.0(-4)	1.961	14.911574	1.2(-4)	1.960	12.954569	5.0(-5)	1.931	38.403

confirm that RBF-FD method needs less time and spatial steps than the method presented in [36], also since both methods lead to the tridiagonal and diagonal dominant matrices, then it is easy to derive that the RBF-FD method is faster than the proposed method in [36]. Also, parameters of this example have been used for numerical approximation of European and American options with finite element scheme in [43]. Comparing the CPU times in second reported in Table 4 with those given in [43] confirms that RBF-FD method is faster than finite element scheme presented in [43].

For convergence analysis of RBF-FD method, we plot maximum error defined by (62) for $S_j \in [Ke^{-3}, Ke^3]$ and different regimes. Analytical solutions for both European and American options are not available, then we use a very accurate

Table 5
Numerical results for American put option under regime switching of Merton model for Example 2.

N_x	M	$S = 90$			$S = 100$			$S = 110$			Time (s)
		Price	Error	Ratio	Price	Error	Ratio	Price	Error	Ratio	
Regime 1											
50	50	14.272457			11.054786			9.197599			0.129
100	100	14.340025	6.7(-2)		11.106532	5.1(-2)		9.223212	2.5(-2)		0.100
200	200	14.358567	1.8(-2)	1.866	11.120249	1.3(-2)	1.916	9.230116	6.9(-3)	1.891	0.263
400	400	14.363438	4.8(-3)	1.929	11.123851	3.6(-3)	1.929	9.231945	1.8(-3)	1.917	0.906
800	800	14.364642	1.2(-3)	2.016	11.124762	9.1(-4)	1.983	9.232411	4.6(-4)	1.970	4.305
1600	1600	14.364933	2.9(-4)	2.048	11.124991	2.2(-4)	1.987	9.232530	1.1(-4)	1.967	42.846
Regime 2											
50	50	16.565212			13.766685			11.853872			0.129
100	100	16.637651	7.2(-2)		13.814636	4.7(-2)		11.875627	2.1(-2)		0.100
200	200	16.657288	1.9(-2)	1.883	13.827081	1.2(-2)	1.946	11.881597	5.9(-3)	1.866	0.263
400	400	16.662406	5.1(-3)	1.940	13.830312	3.2(-3)	1.945	11.883172	1.5(-3)	1.922	0.906
800	800	16.663697	1.2(-3)	1.987	13.831133	8.2(-4)	1.976	11.883574	4.0(-4)	1.971	4.305
1600	1600	16.664017	3.2(-4)	2.010	13.831340	2.0(-4)	1.983	11.883676	1.0(-4)	1.979	42.846
Regime 3											
50	50	18.373931			15.696379			13.670450			0.129
100	100	18.446424	7.2(-2)		15.737293	4.0(-2)		13.688616	1.8(-2)		0.100
200	200	18.465373	1.8(-2)	1.936	15.747919	1.0(-2)	1.945	13.693829	5.2(-3)	1.801	0.263
400	400	18.470273	4.9(-3)	1.951	15.750673	2.7(-3)	1.948	13.695213	1.3(-3)	1.913	0.906
800	800	18.471514	1.2(-3)	1.982	15.751371	6.9(-4)	1.978	13.695565	3.5(-4)	1.975	4.305
1600	1600	18.471823	3.0(-4)	2.002	15.751547	1.7(-4)	1.988	13.695653	8.8(-5)	1.988	42.846

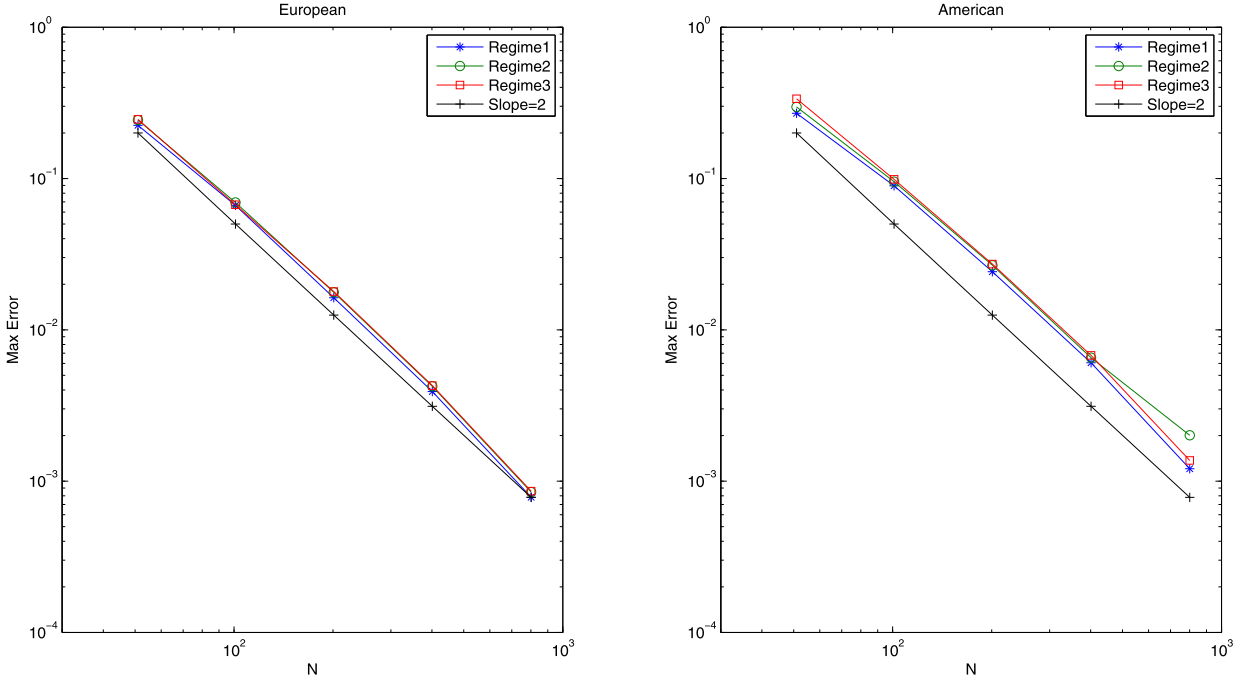

Fig. 5. Left: Error convergence in space for European put option using 1600 time discretization steps. Right: Error convergence in space for American put option using 1600 time discretization steps.

solution obtained by the RBF-FD approximation with a very large number of grid points 3200 and time steps 3200 as $V^{ref}(0, S_j, i)$. Fig. 5 shows the rate of convergence in space for European and American options and confirms the result in Theorem 3.

Example 3. In this example, we consider European and American put option under the regime switching model with parameters chosen from [36]

Table 6
Numerical results for European put option under regime switching of Kou model for Example 3.

N_x	M	$S=90$			$S=100$			$S=110$			Time (s)
		Price	Error	Ratio	Price	Error	Ratio	Price	Error	Ratio	
Regime 1											
50	50	14.906954			9.795429			6.213575			0.539
100	100	14.901212	5.7(-3)		9.789655	5.7(-3)		6.204507	9.0(-3)		0.201
200	200	14.899750	1.4(-3)	1.974	9.788151	1.5(-3)	1.941	6.202214	2.2(-3)	1.983	0.428
400	400	14.899384	3.6(-4)	1.999	9.787772	3.7(-4)	1.989	6.201638	5.7(-4)	1.995	1.680
800	800	14.899290	9.4(-5)	1.961	9.787676	9.6(-5)	1.974	6.201494	1.4(-4)	1.989	14.146
1600	1600	14.899277	1.2(-5)	2.914	9.787666	9.4(-6)	3.350	6.201472	2.1(-5)	2.757	119.123
Regime 2											
50	50	15.448248			10.353514			6.754610			0.139
100	100	15.441654	6.5(-3)		10.347045	6.4(-3)		6.745027	9.5(-3)		0.201
200	200	15.439981	1.6(-3)	1.978	10.345370	1.6(-3)	1.950	6.742606	2.4(-3)	1.985	0.428
400	400	15.439563	4.1(-4)	2.002	10.344949	4.2(-4)	1.993	6.741999	6.0(-4)	1.997	1.680
800	800	15.439457	1.0(-4)	1.972	10.344842	1.0(-4)	1.981	6.741847	1.5(-4)	1.992	14.146
1600	1600	15.439440	1.6(-5)	2.706	10.344830	1.1(-5)	3.161	6.741823	2.3(-5)	2.701	119.123
Regime 3											
50	50	15.980462			10.903399			7.289208			0.139
100	100	15.972947	7.5(-3)		10.896177	7.2(-3)		7.279060	1.0(-2)		0.201
200	200	15.971046	1.9(-3)	1.982	10.894316	1.8(-3)	1.957	7.276499	2.5(-3)	1.986	0.428
400	400	15.970571	4.7(-4)	2.004	10.893850	4.6(-4)	1.996	7.275858	6.4(-4)	1.998	1.680
800	800	15.970451	1.2(-4)	1.981	10.893732	1.1(-4)	1.988	7.275697	1.6(-4)	1.995	14.146
1600	1600	15.970431	1.9(-5)	2.634	10.893716	1.5(-5)	2.943	7.275671	2.5(-5)	2.646	119.123
Regime 4											
50	50	16.503821			11.445235			7.817432			0.139
100	100	16.495317	8.5(-3)		11.437203	8.0(-3)		7.806670	1.0(-2)		0.201
200	200	16.493170	2.1(-3)	1.985	11.435142	2.0(-3)	1.963	7.803957	2.7(-3)	1.988	0.428
400	400	16.492635	5.3(-4)	2.005	11.434627	5.1(-4)	1.998	7.803278	6.7(-4)	1.999	1.680
800	800	16.492500	1.3(-4)	1.989	11.434497	1.2(-4)	1.993	7.803109	1.7(-4)	1.998	14.146
1600	1600	16.492476	2.3(-5)	2.519	11.434478	1.8(-5)	2.790	7.803080	2.8(-5)	2.573	119.123
Regime 5											
50	50	17.018541			11.979170			8.339349			0.139
100	100	17.008983	9.5(-3)		11.970272	8.8(-3)		8.327924	1.1(-2)		0.201
200	200	17.006574	2.4(-3)	1.988	11.967998	2.2(-3)	1.968	8.325047	2.8(-3)	1.989	0.428
400	400	17.005974	5.9(-4)	2.007	11.967430	5.6(-4)	2.000	8.324328	7.1(-4)	2.001	1.680
800	800	17.005824	1.5(-4)	1.995	11.967288	1.4(-4)	1.998	8.324148	1.8(-4)	2.001	14.146
1600	1600	17.005795	2.8(-5)	2.418	11.967265	2.2(-5)	2.643	8.324117	3.0(-5)	2.558	119.123

$$\begin{pmatrix} r_1 \\ r_2 \\ r_3 \\ r_4 \\ r_5 \end{pmatrix} = \begin{pmatrix} 0.05 \\ 0.05 \\ 0.05 \\ 0.05 \\ 0.05 \end{pmatrix}, \quad \begin{pmatrix} \sigma_1 \\ \sigma_2 \\ \sigma_3 \\ \sigma_4 \\ \sigma_5 \end{pmatrix} = \begin{pmatrix} 0.5 \\ 0.5 \\ 0.5 \\ 0.5 \\ 0.5 \end{pmatrix}, \quad \begin{pmatrix} \lambda_1 \\ \lambda_2 \\ \lambda_3 \\ \lambda_4 \\ \lambda_5 \end{pmatrix} = \begin{pmatrix} 0.1 \\ 0.3 \\ 0.5 \\ 0.7 \\ 0.9 \end{pmatrix}$$

$$\mathbf{Q} = \begin{pmatrix} -1 & 0.25 & 0.25 & 0.25 & 0.25 \\ 0.25 & -1 & 0.25 & 0.25 & 0.25 \\ 0.25 & 0.25 & -1 & 0.25 & 0.25 \\ 0.25 & 0.25 & 0.25 & -1 & 0.25 \\ 0.25 & 0.25 & 0.25 & 0.25 & -1 \end{pmatrix}.$$

All regimes have maturity time $T = 0.25$ and exercise price $K = 100$, and jump parameters for Kou density function are $\eta_1 = 3, \eta_2 = 2$, $p = 0.5$ and $q_i = 0$. The results are reported in Tables 6 and 7 at $S = 90, 100, 110$ for different regimes and European and American options with the truncated domain of the log price $[x_{\min}, x_{\max}] = [-1.5, 1.5]$. Comparing results presented in [36] for this set of parameters with RBF-FD method confirms that for getting a specific level of accuracy, RBF-FD technique needs less numbers of time and space steps and therefore RBF-FD will be faster than the method proposed in [36].

Maximum errors defined by (62) for $S_j \in [Ke^{-3}, Ke^3]$ and different regimes are plotted in Fig. 6. Since exact solutions for both European and American options are not available, then we used a very accurate solution obtained by the RBF-FD approximation with a very large number of grid points 3200 and time steps 3200 as $V^{ref}(0, S_j, i)$. Fig. 6 grantees the analytical discussions and shows order of space convergence.

Table 7
Numerical results for American put option under regime switching of Kou model for Example 3.

N_x	M	$S=90$			$S=100$			$S=110$			Time (s)
		Price	Error	Ratio	Price	Error	Ratio	Price	Error	Ratio	
Regime 1											
50	50	15.017425			9.849017			6.242376			0.135
100	100	15.019067	1.6(-3)		9.849967	9.5(-4)		6.235870	6.5(-3)		0.202
200	200	15.019601	5.3(-4)	1.615	9.850214	2.4(-4)	1.943	6.234595	1.2(-3)	2.351	0.428
400	400	15.019783	1.8(-4)	1.547	9.850281	6.7(-5)	1.872	6.234350	2.4(-4)	2.383	1.680
800	800	15.019819	3.6(-5)	2.351	9.850300	1.9(-5)	1.812	6.234298	5.2(-5)	2.234	14.282
1600	1600	15.019839	2.0(-5)	0.847	9.850324	2.4(-5)	0.372	6.234307	9.1(-6)	2.509	120.301
Regime 2											
50	50	15.515114			10.388098			6.773823			0.135
100	100	15.511389	3.7(-3)		10.383251	4.8(-3)		6.765114	8.7(-3)		0.202
200	200	15.510532	8.5(-4)	2.120	10.382074	1.1(-3)	2.042	6.762981	2.1(-3)	2.030	0.428
400	400	15.510304	2.2(-4)	1.910	10.381773	3.0(-4)	1.969	6.762447	5.3(-4)	1.999	1.680
800	800	15.510238	6.7(-5)	1.775	10.381693	8.0(-5)	1.913	6.762312	1.3(-4)	1.983	14.282
1600	1600	15.510228	9.3(-6)	2.830	10.381685	7.0(-6)	3.511	6.762292	1.9(-5)	2.821	120.301
Regime 3											
50	50	16.022729			10.927216			7.304358			0.135
100	100	16.016262	6.4(-3)		10.920520	6.6(-3)		7.294497	9.8(-3)		0.202
200	200	16.014654	1.6(-3)	2.008	10.918826	1.6(-3)	1.983	7.292040	2.4(-3)	2.004	0.428
400	400	16.014256	3.9(-4)	2.014	10.918408	4.1(-4)	2.018	7.291432	6.0(-4)	2.016	1.680
800	800	16.014154	1.0(-4)	1.972	10.918304	1.0(-4)	2.006	7.291282	1.5(-4)	2.017	14.282
1600	1600	16.014139	1.4(-5)	2.844	10.918292	1.1(-5)	3.231	7.291260	2.1(-5)	2.789	120.301
Regime 4											
50	50	16.537290			11.466335			7.832278			0.135
100	100	16.529580	7.7(-3)		11.458797	7.5(-3)		7.821850	1.0(-2)		0.202
200	200	16.527675	1.9(-3)	2.016	11.456903	1.8(-3)	1.993	7.819258	2.5(-3)	2.008	0.428
400	400	16.527209	4.6(-4)	2.032	11.456440	4.6(-4)	2.030	7.818620	6.3(-4)	2.023	1.680
800	800	16.527094	1.1(-4)	2.023	11.456327	1.1(-4)	2.036	7.818464	1.5(-4)	2.031	14.282
1600	1600	16.527077	1.6(-5)	2.780	11.456314	1.2(-5)	3.128	7.818441	2.2(-5)	2.779	120.301
Regime 5											
50	50	17.049874			12.000328			8.354932			0.135
100	100	17.041167	8.7(-3)		11.992018	8.3(-3)		8.343930	1.1(-2)		0.202
200	200	17.039023	2.1(-3)	2.021	11.989940	2.0(-3)	1.999	8.341200	2.7(-3)	2.011	0.428
400	400	17.038502	5.2(-4)	2.042	11.989434	5.0(-4)	2.037	8.340530	6.7(-4)	2.027	1.680
800	800	17.038376	1.2(-4)	2.047	11.989312	1.2(-4)	2.053	8.340368	1.6(-4)	2.041	14.282
1600	1600	17.038357	1.8(-5)	2.746	11.989297	1.4(-5)	3.039	8.340343	2.4(-5)	2.731	120.301

Example 4. In this example, we consider European put option under the four regimes with parameters

$$\begin{pmatrix} r_1 \\ r_2 \\ r_3 \\ r_4 \end{pmatrix} = \begin{pmatrix} 0.02 \\ 0.1 \\ 0.06 \\ 0.15 \end{pmatrix}, \quad \begin{pmatrix} \sigma_1 \\ \sigma_2 \\ \sigma_3 \\ \sigma_4 \end{pmatrix} = \begin{pmatrix} 0.9 \\ 0.5 \\ 0.7 \\ 0.2 \end{pmatrix}, \quad \begin{pmatrix} \lambda_1 \\ \lambda_2 \\ \lambda_3 \\ \lambda_4 \end{pmatrix} = \begin{pmatrix} 8 \\ 2 \\ 5 \\ 1 \end{pmatrix}$$

$$\mathbf{Q} = \begin{pmatrix} -1 & \frac{1}{3} & \frac{1}{3} & \frac{1}{3} \\ \frac{1}{3} & -1 & \frac{1}{3} & \frac{1}{3} \\ \frac{1}{3} & \frac{1}{3} & -1 & \frac{1}{3} \\ \frac{1}{3} & \frac{1}{3} & \frac{1}{3} & -1 \end{pmatrix}.$$

In this case, the market can be in any of the four regimes with equal probability. All options have maturity time $T=1$ and exercise price $K=100$, and jump parameters for Kou density function are $\eta_1=3.0465$, $\eta_2=3.0775$, $p=0.3445$ and for all regimes $q_i=0$, and these parameters are chosen from [22]. Numerical results are reported in Table 8 at $S=92,100,108$ for second and forth regimes and European option with the truncated domain of the log price $[x_{\min},x_{\max}]=[-5,5]$. Comparing the CPU times for RBF-FD method given in Table 8 with two different algorithms presented in [22] given in Table 5 reveals that RBF-FD method is more faster than the algorithms presented in [22] for solving PIDE arisen in pricing European option under regime switching model with jump diffusion process.

Maximum errors for second and fourth regimes and $S_j \in [Ke^{-5}, Ke^{5}]$ are plotted in Fig. (7). Since exact solution for European option is not available, then we used a very accurate solution obtained by the RBF-FD approximation with a very large number of grid points 3200 and time steps 3200 as $V^{ref}(0,S_j,i)$.

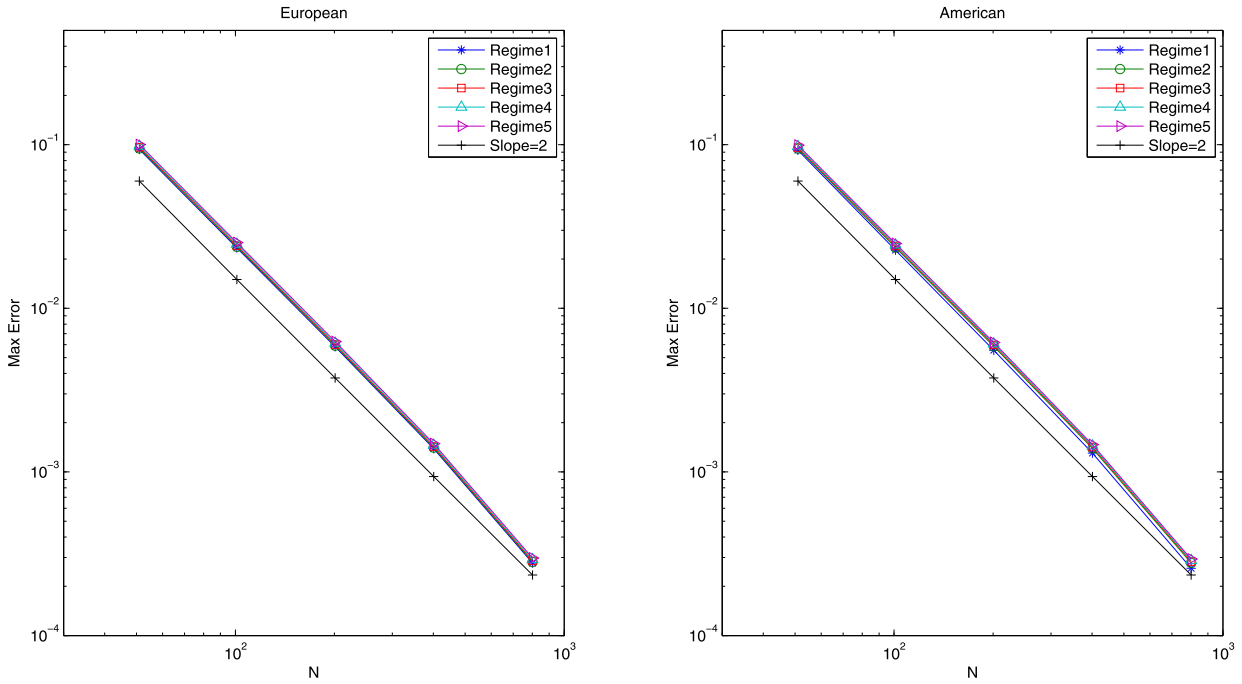

Fig. 6. Left: Error convergence in space for European put option using 1600 time discretization steps. Right: Error convergence in space for American put option using 1600 time discretization steps.

Table 8
Numerical results for European put option under regime switching of Kou model for Example 4.

N_x	M	$S = 92$			$S = 100$			$S = 108$			Time (s)
		Price	Error	Ratio	Price	Error	Ratio	Price	Error	Ratio	
Regime 2											
50	50	32.8235			30.2674			28.0005			0.115
100	100	32.0192	8.0(-1)		29.5138	7.5(-1)		27.2922	7.0(-1)		0.184
200	200	31.8214	1.9(-1)	2.023	29.3285	1.8(-1)	2.024	27.1180	1.7(-1)	2.023	0.398
400	400	31.7722	4.9(-2)	2.007	29.2824	4.6(-2)	2.007	27.0747	4.3(-2)	2.008	1.495
800	800	31.7599	1.2(-2)	1.998	29.2708	1.1(-2)	1.995	27.0639	1.0(-2)	1.996	8.223
1600	1600	31.7568	3.0(-3)	2.004	29.2680	2.8(-3)	2.007	27.0611	2.7(-3)	2.005	67.025
Regime 4											
50	50	24.9835			22.4728			20.4033			0.115
100	100	24.3921	5.9(-1)		21.9291	5.4(-1)		19.8956	5.0(-1)		0.184
200	200	24.2472	1.4(-1)	2.028	21.7959	1.3(-1)	2.029	19.7714	1.2(-1)	2.031	0.398
400	400	24.2111	3.6(-2)	2.005	21.7627	3.3(-2)	2.003	19.7404	3.1(-2)	2.002	1.495
800	800	24.2021	9.0(-3)	2.003	21.7544	8.3(-3)	1.996	19.7327	7.7(-3)	2.009	8.223
1600	1600	24.1998	2.2(-3)	2.003	21.7523	2.0(-3)	2.009	19.7308	1.9(-3)	1.996	67.025

7. Conclusion

In this work, we employed a radial basis function-generated finite differences scheme for European and American option pricing problems under regime switching jump diffusion model. The free boundary problem formulated as a PIDE was transformed into a LCP problem. A RBF-FD approximation was used for the spatial discretization, and then, three time levels are considered for time discretization which were combined with an operator splitting method. These result in a linear algebraic system with a sparse matrix. Also, we prove that the coefficient matrix of the linear system of equations is tridiagonal and diagonal dominant. To overcome the discontinuity issue near the strike price for derivatives of payoff function, average value of the payoff function over the surrounding grids rather than its value sampled at each grid point is considered and this makes the payoff function smooth at the strike price K, and by using this technique we make some improvements in the accuracy of RBF-FD method especially near the strike price. Convergence theorems confirms theoretically the accuracy of RBF-FD approximation combined with three time level of discretization, and numerical results reported in some tables and figures grantee this fact numerically.

Parameter set of the first example has been considered in [43] by finite element method and in [15] by multinomial lattice approach. Comparing the results confirms that RBF-FD method combined with an stable three level time discretization

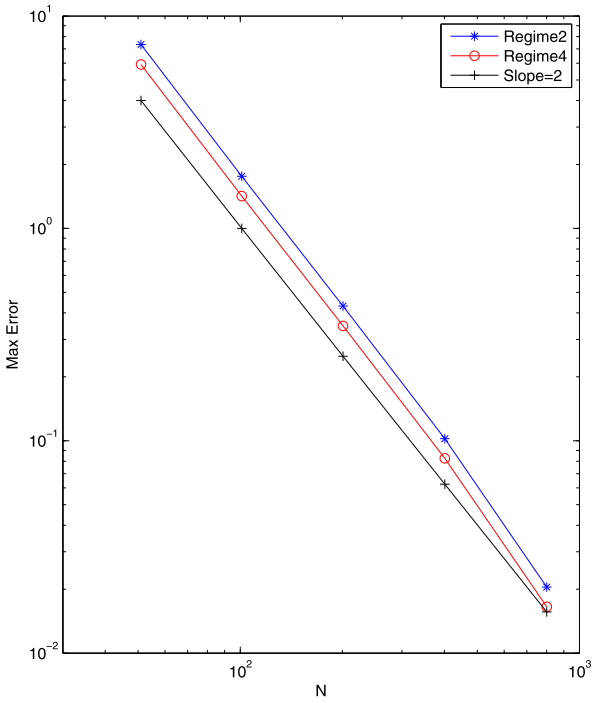

Fig. 7. Error convergence in space for European put option using 1600 time discretization steps.

for European option and operator splitting method for American option is accurate and faster that finite element method and multinomial lattice approach. To show the efficiency of RBF-FD method for different kind of parameter values, we considered large values for jump intensity and high volatility in Example 1 and numerical results show that the proposed numerical scheme gives good accuracy for high volatility and large jump intensity as well as small values and for both European and American put option prices. Presented results show that RBF-FD technique needs less time and space steps for reaching an specific level of accuracy than classical finite difference method [36].

References

[1] L. Andersen, Markov models for commodity futures: theory and practice, Quant. Finance 10 (8) (2010) 831–854.
[2] U.M. Ascher, S.J. Ruuth, B.T.R. Wetton, Implicit-explicit methods for time-dependent partial differential equations, SIAM J. Numer. Anal. 32 (3) (1995) 797–823.
[3] Luca Vincenzo Ballestra, Liliana Cecere, A fast numerical method to price American options under the Bates model, Comput. Math. Appl. 72 (5) (2016) 1305–1319.
[4] L.V. Ballestra, G. Pacelli, Pricing European and American options with two stochastic factors: a highly efficient radial basis function approach, J. Econ. Dyn. Control 37 (6) (2013) 1142–1167.
[5] Luca Vincenzo Ballestra, Carlo Sgarra, The evaluation of American options in a stochastic volatility model with jumps: an efficient finite element approach, Comput. Math. Appl. 60 (6) (2010) 1571–1590.
[6] R. Bansal, H. Zhou, Term structure of interest rates with regime shifts, J. Finance 57 (5) (2002) 1997–2043.
[7] A.F. Bastani, Z. Ahmadi, D. Damircheli, A radial basis collocation method for pricing American options under regime-switching jump-diffusion models, Appl. Numer. Math. 65 (2013) 79–90.
[8] V. Bayona, M. Moscoso, M. Carretero, M. Kindelan, RBF-FD formulas and convergence properties, J. Comput. Phys. 229 (22) (2010) 8281–8295.
[9] F. Black, M. Scholes, The pricing of options and corporate liabilities, J. Polit. Econ. 81 (3) (1973) 637–654.
[10] A. Borici, H.-J. Lüthi, Pricing American put options by fast solutions of the linear complementarity problem, in: E.J. Kontoghiorghes, B. Rustem, S. Siokos (Eds.), Computational Methods in Decision-Making, Economics and Finance, Springer, US, 2002, pp. 325–338.
[11] J. Buffington, R.J. Elliott, American options with regime switching, Int. J. Theor. Appl. Finance 05 (05) (2002) 497–514.
[12] P. Carr, H. Geman, The fine structure of asset returns: an empirical investigation, J. Bus. 75 (2) (2002) 305–332.
[13] Z. Chen, P.A. Forsyth, Implications of a regime-switching model on natural gas storage valuation and optimal operation, Quant. Finance 10 (2) (2010) 159–176.
[14] C. Chiarella, B. Kang, G.H. Meyer, A. Ziogas, The evaluation of American option prices under stochastic volatility and jump-diffusion dynamics using the method of lines, Int. J. Theor. Appl. Finance 12 (03) (2009) 393–425.
[15] M. Costabile, A. Leccadito, I. Massabó, E. Russo, Option pricing under regime-switching jump–diffusion models, J. Comput. Appl. Math. 256 (2014) 152–167.
[16] R.J. Elliott, L. Chan, T.K. Siu, Option pricing and Esscher transform under regime switching, Ann. Finance 1 (4) (2005) 423–432.
[17] P. Eloe, R.H. Liu, Upper and lower solutions for regime-switching diffusions with applications in financial mathematics, SIAM J. Appl. Math. 71 (4) (2011) 1354–1373.
[18] P. Eloe, R.H. Liu, M. Yatsuki, G. Yin, Q. Zhang, Optimal selling rules in a regime-switching exponential Gaussian diffusion model, SIAM J. Appl. Math. 69 (3) (2008) 810–829.

[19] M. Fakharany, R. Company, L. Jódar, Positive finite difference schemes for a partial integro-differential option pricing model, Appl. Math. Comput. 249 (2014) 320–332.
[20] G.E. Fasshauer, A.Q.M. Khaliq, D.A. Voss, Using meshfree approximation for multiasset American options, J. Chin. Inst. Eng. 27 (4) (2004) 563–571.
[21] I. Florescu, R. Liu, M.C. Mariani, Solutions to a partial integro-differential parabolic system arising in the pricing of financial options in regime-switching jump diffusion models, Electron. J. Differ. Equ. 2012 (231) (2012) 1–12.
[22] I. Florescu, R. Liu, M.C. Mariani, G. Sewell, Numerical schemes for option pricing in regime-switching jump diffusion models, Int. J. Theor. Appl. Finance 16 (08) (2013) 1350046.
[23] B. Fornberg, N. Flyer, A Primer on Radial Basis Functions with Applications to the Geosciences, SIAM, Philadelphia, 2015.
[24] B. Fornberg, N. Flyer, Solving PDEs with radial basis functions, Acta Numer. 24 (2015) 215–258.
[25] P.A. Gagniuc, Markov Chains: From Theory to Implementation and Experimentation, John Wiley & Sons, Inc., NJ, USA, 2017.
[26] X. Guo, Information and option pricings, Quant. Finance 1 (1) (2001) 38–44.
[27] N. Haldrup, M.O. Nielsen, A regime switching long memory model for electricity prices, J. Econom. 135 (1–2) (2006) 349–376.
[28] M. Hardy, A regime-switching model of long-term stock returns, N. Am. Actuar. J. 5 (2) (2001) 41–53.
[29] S. Ikonen, J. Toivanen, Operator splitting methods for American option pricing, Appl. Math. Lett. 17 (7) (2004) 809–814.
[30] S. Ikonen, J. Toivanen, Operator splitting methods for pricing American options under stochastic volatility, Numer. Math. 113 (2) (2009) 299–324.
[31] M.K. Kadalbajoo, L.P. Tripathi, A. Kumar, Second order accurate IMEX methods for option pricing under Merton and Kou jump-diffusion models, J. Sci. Comput. 65 (3) (2015) 979–1024.
[32] A. Kanas, On real interest rate dynamics and regime switching, J. Bank. Finance 32 (10) (2008) 2089–2098.
[33] A.Q.M. Khaliq, R.H. Liu, New numerical scheme for pricing American option with regime-switching, Int. J. Theor. Appl. Finance 12 (03) (2009) 319–340.
[34] S.G. Kou, A jump-diffusion model for option pricing, Manag. Sci. 48 (8) (2002) 1086–1101.
[35] Y. Kwon, Y. Lee, A second-order finite difference method for option pricing under jump-diffusion models, SIAM J. Numer. Anal. 49 (6) (2011) 2598–2617.
[36] Y. Lee, Financial options pricing with regime-switching jump-diffusions, Comput. Math. Appl. 68 (3) (2014) 392–404.
[37] R.H. Liu, Regime-switching recombining tree for option pricing, Int. J. Theor. Appl. Finance 13 (03) (2010) 479–499.
[38] R.H. Liu, J.L. Zhao, A lattice method for option pricing with two underlying assets in the regime-switching model, J. Comput. Appl. Math. 250 (2013) 96–106.
[39] R. Merton, Option pricing when underlying stock returns are discontinuous, J. Financ. Econ. 3 (1–2) (1976) 125–144.
[40] R. Mollapourasl, A. Fereshtian, H. Li, X. Lu, RBF-PU method for pricing options under the jump-diffusion model with local volatility, J. Comput. Appl. Math. 337 (2018) 98–118.
[41] R. Mollapourasl, A. Fereshtian, M. Vanmaele, Radial basis functions with partition of unity method for American options with stochastic volatility, Comput. Econ. (Sep 2017) 1–29.
[42] D.M. Pooley, K.R. Vetzal, P.A. Forsyth, Convergence remedies for non-smooth payoffs in option pricing, J. Comput. Finance 6 (4) (2003) 25–40.
[43] N. Rambeerich, A.A. Pantelous, A high order finite element scheme for pricing options under regime switching jump diffusion processes, J. Comput. Appl. Math. 300 (2016) 83–96.
[44] A. Safdari-Vaighani, A. Heryudono, E. Larsson, A radial basis function partition of unity collocation method for convection–diffusion equations arising in financial applications, J. Sci. Comput. 64 (2) (2015) 341–367.
[45] S. Salmi, J. Toivanen, IMEX schemes for pricing options under jump-diffusion models, Appl. Numer. Math. 84 (2014) 33–45.
[46] R. Seydel, Tools for Computational Finance, 4th edition, Springer, Berlin, Heidelberg, 2009.
[47] V. Shcherbakov, E. Larsson, Radial basis function partition of unity methods for pricing vanilla basket options, Comput. Math. Appl. 71 (1) (2016) 185–200.
[48] M.I.M. Wahab, Z. Yin, N.C.P. Edirisinghe, Pricing swing options in the electricity markets under regime-switching uncertainty, Quant. Finance 10 (9) (2010) 975–994.
[49] H. Wendland, Scattered Data Approximation, Cambridge Monographs on Applied and Computational Mathematics, vol. 17, Cambridge University Press, New York, 2005.
[50] G. Yin, Q. Zhang, Continuous-Time Markov Chains and Applications: A Singular Perturbation Approach, Springer, 1998.
[51] M. Yousuf, A.Q.M. Khaliq, R.H. Liu, Pricing American options under multi-state regime switching with an efficient L-stable method, Int. J. Comput. Math. 92 (12) (2015) 2530–2550.
[52] F.L. Yuen, H. Yang, Option pricing with regime switching by trinomial tree method, J. Comput. Appl. Math. 233 (8) (2010) 1821–1833.
[53] Q. Zhang, X.Y. Zhou, Valuation of stock loans with regime switching, SIAM J. Control Optim. 48 (3) (2009) 1229–1250.
[54] R. Zvan, P.A. Forsyth, K.R. Vetzal, Penalty methods for American options with stochastic volatility, J. Comput. Appl. Math. 91 (2) (1998) 199–218.